Two-loop renormalization of vector, axial-vector and tensor fermion bilinears on the lattice

A. Skouroupathis and H. Panagopoulos

Department of Physics, University of Cyprus,

P.O. Box 20537, Nicosia CY-1678, Cyprus

email: `php4as01@ucy.ac.cy, haris@ucy.ac.cy`

(Dated: April 24, 2009)

Abstract

We compute the two-loop renormalization functions, in the RI' scheme, of local bilinear quark operators $\bar{\psi}\Gamma\psi$, where Γ corresponds to the Vector, Axial-Vector and Tensor Dirac operators, in the lattice formulation of QCD. We consider both the flavor nonsinglet and singlet operators.

We use the clover action for fermions and the Wilson action for gluons. Our results are given as a polynomial in c_{SW}, in terms of both the renormalized and bare coupling constant, in the renormalized Feynman gauge.

Finally, we present our results in the $\overline{MS}$ scheme, for easier comparison with calculations in the continuum. The corresponding results, for fermions in an *arbitrary* representation, together with some special features of superficially divergent integrals, are included in the Appendices.

I.   INTRODUCTION

Numerical simulations of QCD, formulated on the lattice, make use of a variety of composite operators, made out of quark fields. In particular, matrix elements and correlation functions of such operators, which include local and extended bilinears, as well as four-fermion operators, are computed in order to study hadronic properties in this context. A proper renormalization of these operators is essential for the extraction of physical results from the dimensionless quantities measured in numerical simulations.

The present paper is the second in a series of papers regarding the calculation of renormalization functions of fermion bilinear operators to two loops in Lattice perturbation theory. The calculation of the scalar and pseudoscalar cases was carried out in Ref. [1]. In this work we study the renormalization function Z_Γ of fermion bilinears $\mathcal{O} = \bar{\psi}\Gamma\psi$ on the lattice, where $\Gamma = \gamma_\mu$, $\gamma_5\,\gamma_\mu$, $\gamma_5\,\sigma_{\mu\nu}$ ($\sigma_{\mu\nu} = 1/2\,[\gamma_\mu, \gamma_\nu]$). We consider both flavor singlet and nonsinglet operators. We employ the standard Wilson action for gluons and clover-improved Wilson fermions. The number of quark flavors N_f, the number of colors N_c and the clover coefficient c_{SW} are kept as free parameters. One necessary ingredient for the renormalization of fermion bilinears is the 2-loop quark field renormalization, Z_ψ, calculated in [1]. The one-loop expression for the renormalization function Z_g of the coupling constant is also necessary for expressing the results in terms of both the bare and the renormalized coupling constant.

Our two-loop calculations have been performed in the bare and in the renormalized Feynman gauge. For the latter, we need the 1-loop renormalization functions Z_α and Z_A of the gauge parameter and gluon field respectively, as well as the one-loop expressions for Z_Γ with an arbitrary value of the gauge parameter.

The main results presented in this work are the following 2-loop bare Green's functions (amputated, one-particle irreducible (1PI)):

- 2-pt function of the vector operator $\bar{\psi}\gamma_\mu\psi$: $\Sigma_V^L(qa_{\mathrm{L}})$

- 2-pt function of the axial-vector operator $\bar{\psi}\gamma_5\gamma_\mu\psi$: $\Sigma_{AV}^L(qa_{\mathrm{L}})$

- 2-pt function of the tensor operator $\bar{\psi}\gamma_5\sigma_{\mu\nu}\psi$: $\Sigma_T^L(qa_{\mathrm{L}})$

(a_{L} : lattice spacing, q : external momentum).

In general, one can use bare Green's functions to construct $Z_\mathcal{O}^{X,Y}$, the renormalization function for operator $\mathcal{O}$, computed within a regularization X ($X = L$: lattice regularization;

$X = DR$: dimensional regularization) and renormalized in a scheme Y. We employ two widely used schemes to compute the various two-loop renormalization functions:

- The RI' scheme: $Z_V^{L,RI'}$, $Z_{AV}^{L,RI'}$, $Z_T^{L,RI'}$

- The $\overline{MS}$ scheme: $Z_V^{L,\overline{MS}}$, $Z_{AV}^{L,\overline{MS}}$, $Z_T^{L,\overline{MS}}$

For convenience, the results for $Z_{\mathcal{O}}^{X,Y}$ are given in terms of both the bare coupling constant g_o and the renormalized one: $g_{RI'}$, $g_{\overline{MS}}$. Finally, as one of several checks on our results, we construct the 2-loop renormalized Green's functions in RI': $\Sigma_{\mathcal{O}}^{RI'}(q,\bar{\mu})$ ($\mathcal{O} \equiv V, AV, T$), as well as their counterparts in $\overline{MS}$: $\Sigma_{\mathcal{O}}^{\overline{MS}}(q,\bar{\mu})$. The values of all these functions, computed on the lattice, coincide with values computed in dimensional regularization (we derive the latter from the results of Ref. [2]).

The present work, along with [1], is the first two-loop computation of the renormalization of fermion bilinears on the lattice. One-loop computations of the same quantities exist for quite some time now (see, e.g., [3], [4], [5] and references therein). There have been made several attempts to estimate $Z_{\mathcal{O}}$ non-perturbatively; recent results can be found in Refs. [6, 7, 8, 9, 10, 11]. A series of results have also been obtained using stochastic perturbation theory [12, 13, 14]. A related computation, regarding the fermion mass renormalization Z_m with staggered fermions can be found in [15].

The paper is organized as follows: Section II provides a formulation of the problem, as well as all necessary definitions of renormalization schemes and of the quantities to compute. Section III describes our computational methods and results. Finally, in Section IV we discuss some salient features of our calculation, and comment on future extensions to the present work.

Recently, there has been some interest in gauge theories with fermions in different representations [16] of the gauge group. Such theories are being studied in various contexts [17, 18, 19, 20, 21, 22], e.g., supersymmetry [23], phase transitions [24], and the AdS/QCD correspondence. It is relatively straightforward to generalize our results to an arbitrary representation; this is presented in Appendix A. Some special features of 2-, 3- and 4-index superficially divergent integrals are described in Appendix B. Finally, a detailed presentation of our calculation results on a per diagram basis, is provided in Appendix C.

II.   FORMULATION OF THE PROBLEM

A.   Lattice action

In the present work we employ the Wilson formulation of the QCD action on the lattice, with the addition of the clover (SW) [25] term for fermions. In standard notation, it reads:

$$
\begin{aligned}
S_L \;=\; & S_G + \sum_f \sum_x (4r + m_{\mathrm{o}}) \bar{\psi}_f(x) \psi_f(x) \\
& - \frac{1}{2} \sum_f \sum_{x,\mu} \Big[\bar{\psi}_f(x) \, (r - \gamma_\mu) \, U_{x,x+\mu} \, \psi_f(x+\mu) \\
& \qquad\qquad + \bar{\psi}_f(x+\mu) \, (r + \gamma_\mu) \, U_{x+\mu,x} \, \psi_f(x) \Big] \\
& + \frac{i}{4} \, c_{\mathrm{SW}} \sum_f \sum_{x,\mu,\nu} \bar{\psi}_f(x) \, \sigma_{\mu\nu} \, \hat{F}_{\mu\nu}(x) \, \psi_f(x),
\end{aligned}
\tag{1}
$$

$$
\text{where}: \quad \hat{F}_{\mu\nu} \equiv \frac{1}{8a^2} \left(Q_{\mu\nu} - Q_{\nu\mu} \right)
\tag{2}
$$

$$
\begin{aligned}
\text{and}: \quad Q_{\mu\nu} \;=\; & U_{x,x+\mu} \, U_{x+\mu,x+\mu+\nu} \, U_{x+\mu+\nu,x+\nu} \, U_{x+\nu,x} \\
& + U_{x,x+\nu} \, U_{x+\nu,x+\nu-\mu} \, U_{x+\nu-\mu,x-\mu} \, U_{x-\mu,x} \\
& + U_{x,x-\mu} \, U_{x-\mu,x-\mu-\nu} \, U_{x-\mu-\nu,x-\nu} \, U_{x-\nu,x} \\
& + U_{x,x-\nu} \, U_{x-\nu,x-\nu+\mu} \, U_{x-\nu+\mu,x+\mu} \, U_{x+\mu,x}
\end{aligned}
\tag{3}
$$

S_G is the standard pure gluon action, made out of $1{\times}1$ plaquettes. The clover coefficient c_{SW} is treated here as a free parameter; r is the Wilson parameter (set to $r = 1$ henceforth); f is a flavor index; $\sigma_{\mu\nu} = (i/2)[\gamma_\mu, \gamma_\nu]$. Powers of the lattice spacing a_{L} have been omitted and may be directly reinserted by dimensional counting.

The "Lagrangian mass" m_{o} is a free parameter here. However, since we will be using mass independent renormalization schemes, all renormalization functions which we will be calculating, must be evaluated at vanishing renormalized mass, that is, when m_{o} is set equal to the critical value m_{cr}: $m_{\mathrm{o}} \to m_{\mathrm{cr}} = m_1 \, g_{\mathrm{o}}^2 + \mathcal{O}(g_{\mathrm{o}}^4)$.

B.   Definition of renormalized quantities

As a prerequisite to our programme, we will use the renormalization functions, Z_A, Z_c, Z_ψ, Z_g and Z_α, for the gluon, ghost and fermion fields (A_μ^a, c^a, ψ), and for the coupling

constant g and gauge parameter α, respectively (for definitions of these quantities, see Ref. [1]); we will also need the fermion mass counterterm m_{cr}. These quantities are all needed to one loop, except for Z_ψ which is required to two loops. The value of each $Z_{\mathcal{O}}$ depends both on the regularization X and on the renormalization scheme Y employed, and thus should properly be denoted as $Z_{\mathcal{O}}^{X,Y}$.

Our one-loop results for the Vector and Axial-Vector operators, even though performed in a generic gauge, turn out to be independent of the gauge parameter. These results along with the one-loop expression for the Tensor operator, are in agreement with results found in the literature (see, e.g., Ref. [5]).

As mentioned before, we employ the RI' renormalization scheme [26, 27, 28], which is more immediate for a lattice regularized theory. It is defined by imposing a set of normalization conditions on matrix elements at a scale $\bar{\mu}$, where (just as in the $\overline{MS}$ scheme) [29]:

$$\bar{\mu} = \mu \, (4\pi/e^{\gamma_{\mathrm{E}}})^{1/2} \tag{4}$$

where γ_{E} is the Euler constant and μ is the scale entering the bare coupling constant $g_\circ = \mu^\epsilon Z_g \, g$ when regularizing in $D = 4 - 2\epsilon$ dimensions.

C. Conversion to the $\overline{MS}$ scheme

For easier comparison with calculations coming from the continuum, we need to express our results in the $\overline{MS}$ scheme. Each renormalization function on the lattice, $Z_{\mathcal{O}}^{L,RI'}$, may be expressed as a power series in the renormalized coupling constant $g_{RI'}$. For the purposes of our work the conversion of $g_{RI'}$ to $\overline{MS}$ is trivial since:

$$g_{RI'} = g_{\overline{MS}} + \mathcal{O}\left((g_{\overline{MS}})^9\right) \tag{5}$$

The conversion of the gauge parameter $\alpha_{RI'}$ to the $\overline{MS}$ scheme is given by [30]:

$$\alpha_{RI'} = \frac{Z_A^{L,\overline{MS}}}{Z_A^{L,RI'}} \, \alpha_{\overline{MS}} \equiv \alpha_{\overline{MS}} \, / \, C_A(g_{\overline{MS}}, \alpha_{\overline{MS}}) \tag{6}$$

where the conversion factor C_A may be calculated more easily in dimensional regularization (DR) [2], since the ratio of Z's appearing in Eq. (6) is necessarily *regularization independent.*

To one loop, the conversion factor C_A equals:

$$C_A(g, \alpha) = \frac{Z_A^{DR,RI'}}{Z_A^{DR,\overline{MS}}} = 1 + \frac{g^2}{36(16\pi^2)} \left[\left(9\alpha^2 + 18\alpha + 97\right) N_c - 40 N_f\right] \tag{7}$$

(Here, and throughout the rest of this work, both g and α are in the $\overline{MS}$ scheme, unless specified otherwise.)

Once we have computed the renormalized Green's functions in the RI' scheme, we can construct their $\overline{MS}$ counterparts using the quark field conversion factor which, up to the required perturbative order, is given by:

$$
\begin{aligned}
C_\psi(g, \alpha) &\equiv \frac{Z_\psi^{L,RI'}}{Z_\psi^{L,\overline{MS}}} = \frac{Z_\psi^{DR,RI'}}{Z_\psi^{DR,\overline{MS}}} \\
&= 1 - \frac{g^2}{16\pi^2} c_F \, \alpha + \frac{g^4}{8 \, (16\pi^2)^2} c_F \Big[\left(8\alpha^2 + 5\right) c_F + 14 \, N_f \\
&\qquad\qquad - \left(9\alpha^2 - 24\zeta(3)\,\alpha + 52\alpha - 24\zeta(3) + 82\right) N_c \Big] (8)
\end{aligned}
$$

where $c_F = (N_c^2 - 1)/(2 \, N_c)$ is the quadratic Casimir operator in the fundamental representation of the color group; $\zeta(x)$ is Riemann's zeta function.

D.   Renormalization of fermion bilinears

The lattice operators $\mathcal{O}_\Gamma = \bar{\psi} \, \Gamma \, \psi$ must, in general, be renormalized in order to have finite matrix elements. We define renormalized operators by

$$\mathcal{O}_\Gamma^{RI'} = Z_\Gamma^{L,RI'}(a_{\rm L} \bar{\mu}) \, \mathcal{O}_{\Gamma\,{\rm o}} \tag{9}$$

The flavor singlet axial-vector Green's function receives additional contributions as compared to the nonsinglet case, while for the rest of the operators under study, singlet and nonsinglet Green's functions coincide. For the vector (V), axial-vector (AV) and tensor (T) operators, the renormalization functions $Z_\Gamma^{L,RI'}$ can be extracted through the corresponding bare 2-point functions $\Sigma_\Gamma^L(qa_{\rm L})$ (amputated, 1PI) on the lattice. Let us first express these bare Green's functions in the following way:

$$\Sigma_V^L(qa_{\rm L}) = \gamma_\mu \, \Sigma_V^{(1)}(qa_{\rm L}) + \frac{q^\mu \slashed{q}}{q^2} \Sigma_V^{(2)}(qa_{\rm L})$$

6

$$\Sigma_{AV}^{L}(qa_{\mathrm{L}}) = \gamma_5\gamma_\mu \, \Sigma_{AV}^{(1)}(qa_{\mathrm{L}}) + \gamma_5\frac{q^\mu \slashed{q}}{q^2}\Sigma_{AV}^{(2)}(qa_{\mathrm{L}}) \tag{10}$$

$$\Sigma_{T}^{L}(qa_{\mathrm{L}}) = \gamma_5\,\sigma_{\mu\nu}\Sigma_{T}^{(1)}(qa_{\mathrm{L}}) + \gamma_5\frac{\slashed{q}\,(\gamma_\mu q_\nu - \gamma_\nu q_\mu)}{q^2}\Sigma_{T}^{(2)}(qa_{\mathrm{L}})$$

It is worth noting here that terms which break Lorentz invariance (but are compatible with hypercubic invariance), such as $\gamma_\mu\,(q^\mu)^2/q^2$, turn out to be absent from all bare Green's functions; thus, the latter have the same Lorentz structure as in the continuum. Let us also point out that the presence of the γ_5 matrix in the tensor operator definition does not affect the bare Green's function on the lattice, in the RI' scheme. We have performed the calculation both with and without the inclusion of the γ_5 matrix, and we ended up with identical 2-point functions. Thus, for the purpose of converting our results to the $\overline{MS}$ scheme, we employed the conversion factors given in Ref. [2], where the definition of the tensor operator does not contain the γ_5 matrix. Furthermore, we expect that $\Sigma_{T}^{(2)}(qa_{\mathrm{L}})$ must vanish, since this is the case for the corresponding quantity coming from the continuum. Indeed, after performing the calculation on the lattice, it turns out that all contributions of this type vanish.

Once all necessary Feynman diagrams contributing to the bare Green's functions presented above are evaluated, one can obtain the renormalization functions for the three operators through the following conditions:

$$\lim_{a_{\mathrm{L}}\to 0}\left[Z_\psi^{L,RI'}\, Z_V^{L,RI'}\,\Sigma_V^{(1),\,L}(qa_{\mathrm{L}})\right]_{q^2=\bar{\mu}^2} = \gamma_\mu \tag{11}$$

$$\lim_{a_{\mathrm{L}}\to 0}\left[Z_\psi^{L,RI'}\, Z_{AV}^{L,RI'}\,\Sigma_{AV}^{(1),\,L}(qa_{\mathrm{L}})\right]_{q^2=\bar{\mu}^2} = \gamma_5\,\gamma_\mu \tag{12}$$

$$\lim_{a_{\mathrm{L}}\to 0}\left[Z_\psi^{L,RI'}\, Z_T^{L,RI'}\,\Sigma_T^{(1),\,L}(qa_{\mathrm{L}})\right]_{q^2=\bar{\mu}^2} = \gamma_5\,\sigma_{\mu\nu} \tag{13}$$

where:

$$\Sigma_V^{(1)}(qa_{\mathrm{L}}) = 1+\mathcal{O}(g_\circ^2) \quad , \quad \Sigma_V^{(2)}(qa_{\mathrm{L}}) = \mathcal{O}(g_\circ^2)$$

$$\Sigma_{AV}^{(1)}(qa_{\mathrm{L}}) = 1+\mathcal{O}(g_\circ^2) \quad , \quad \Sigma_{AV}^{(2)}(qa_{\mathrm{L}}) = \mathcal{O}(g_\circ^2) \tag{14}$$

$$\Sigma_T^{(1)}(qa_{\mathrm{L}}) = 1+\mathcal{O}(g_\circ^2) \quad , \quad \Sigma_T^{(2)}(qa_{\mathrm{L}}) = 0$$

The conversion of the quantities $Z_\Gamma^{L,RI'}$ to the $\overline{MS}$ scheme is a straightforward procedure. In the case of the vector and tensor operators, the renormalization functions, $Z_V^{L,\overline{MS}}$ and

$Z_T^{L,\overline{MS}}$, can be obtained by:

$$Z_\Gamma^{L,\overline{MS}} = Z_\Gamma^{L,RI'}/C_\Gamma(g,\alpha) \tag{15}$$

where $C_\Gamma(g,\alpha)$ are *regularization independent* conversion factors ($\Gamma = V, T$). These conversion factors have been calculated in dimensional regularization [2]:

$$C_V(g,\alpha) \equiv \frac{Z_V^{L,RI'}}{Z_V^{L,\overline{MS}}} = \frac{Z_V^{DR,RI'}}{Z_V^{DR,\overline{MS}}} = 1 + \mathcal{O}(g^8) \tag{16}$$

$$
\begin{aligned}
C_T(g,\alpha) \equiv{}& \frac{Z_T^{L,RI'}}{Z_T^{L,\overline{MS}}} = \frac{Z_T^{DR,RI'}}{Z_T^{DR,\overline{MS}}} \\
={}& 1 + \frac{g^2}{16\pi^2}\, c_F\, \alpha + \frac{g^4}{216\,(16\pi^2)^2}\, c_F \left[\left(216\alpha^2 + 4320\zeta(3) - 4815\right)\, c_F - 626\, N_f \right. \\
&\left. + \left(162\alpha^2 + 756\alpha - 3024\zeta(3) + 5987\right)\, N_c \right] (17)
\end{aligned}
$$

Unlike the tensor operator, where the presence of the γ_5 matrix is irrelevant, the axial-vector bilinear ($\mathcal{O}_{AV}^\circ = \bar{\psi}_\circ \gamma_5 \gamma_\mu \psi_\circ$) requires special attention also in the $\overline{MS}$ scheme, due to the non-unique generalization of γ_5 to D dimensions. A practical definition of γ_5 for multiloop calculations, which is most commonly employed in dimensional regularization and does not suffer from inconsistencies is [31]:

$$\gamma_5 = i\,\frac{1}{4!}\,\epsilon^{\nu_1\nu_2\nu_3\nu_4}\,\gamma_{\nu_1}\,\gamma_{\nu_2}\,\gamma_{\nu_3}\,\gamma_{\nu_4} \quad, \quad \nu_i = 0,\,1,\,2,\,3 \tag{18}$$

Of course, γ_5 as defined in Eq. (18) does not anticommute (in D dimensions) with γ_μ, for $\mu \geq 4$; an ultimate consequence of this fact is that Ward identities involving the axial-vector and pseudoscalar operators, renormalized in this way, are violated.

To obtain a correctly normalized axial-vector operator [32], $\mathcal{O}_{AV}^{\overline{MS}'}$, one must introduce an extra *finite* factor, Z_5, in addition to the usual renormalization function $Z_{AV}^{DR,\overline{MS}}$ (the latter only contains poles in ϵ). We set:

$$\mathcal{O}_{AV}^{\overline{MS}'} = Z_5(g)\,\mathcal{O}_{AV}^{\overline{MS}} = Z_5(g)\,Z_{AV}^{DR,\overline{MS}}\,\mathcal{O}_{AV}^\circ \tag{19}$$

For the definition of Z_5 we must express the $\overline{MS}$ renormalized Green's functions $G_V^{\overline{MS}}$, $G_{AV}^{\overline{MS}}$ as well as the renormalized Green's function $G_{AV}^{\overline{MS}'}$ (corresponding to $\mathcal{O}_{AV}^{\overline{MS}'}$), in a form similar to Eq. (11):

$$G_V^{\overline{MS}}(qa_{\mathrm{L}}) = \gamma_\mu\, G_V^{(1)\,\overline{MS}}(qa_{\mathrm{L}}) + \frac{q^\mu \slashed{q}}{q^2} G_V^{(2)\,\overline{MS}}(qa_{\mathrm{L}})$$

$$G_{AV}^{\overline{MS}}(qa_{\text{L}}) \;=\; \gamma_5\gamma_\mu\, G_{AV}^{(1)\,\overline{MS}}(qa_{\text{L}}) + \gamma_5 \frac{q^\mu \slashed{q}}{q^2} G_{AV}^{(2)\,\overline{MS}}(qa_{\text{L}}) \tag{20}$$

$$G_{AV}^{\overline{MS}\,\prime}(qa_{\text{L}}) \;=\; \gamma_5\,\sigma_{\mu\nu} G_{AV}^{(1)\,\overline{MS}\,\prime}(qa_{\text{L}}) + \gamma_5 \frac{\slashed{q}\,(\gamma_\mu q_\nu - \gamma_\nu q_\mu)}{q^2} G_{AV}^{(2)\,\overline{MS}\,\prime}(qa_{\text{L}})$$

Z_5 is then defined by the requirement that the renormalized Green's functions $G_V^{(1)\,\overline{MS}}(qa_{\text{L}})$ and $G_{AV}^{(1)\,\overline{MS}\,\prime}(qa_{\text{L}})$ coincide:

$$Z_5 \equiv \frac{G_V^{(1)\,\overline{MS}}}{G_{AV}^{(1)\,\overline{MS}}} \tag{21}$$

Eq.(19) is valid for both the singlet and nonsinglet currents, provided of course, the appropriate choice for Z_5 is used. Thus, we have two different expressions, Z_5^s and Z_5^{ns} corresponding to the singlet and nonsinglet axial-vector operator, respectively. They are gauge independent and differ only in the $c_F\,N_f$ term; this is expected considering the fact that the additional Feynman diagrams contributing to the singlet axial operator have the insertion within the closed fermion loop. Both Z_5^s and Z_5^{ns} were evaluated in DR [32] and up to two loops they read:

$$Z_5^s(g) \;=\; 1 - \frac{g^2}{16\pi^2}\,(4\,c_F) + \frac{g^4}{(16\pi^2)^2}\left(22\,c_F^2 - \frac{107}{9}\,c_F\,N_c + \frac{31}{18}\,c_F\,N_f\right) \tag{22}$$

$$Z_5^{ns}(g) \;=\; 1 - \frac{g^2}{16\pi^2}\,(4\,c_F) + \frac{g^4}{(16\pi^2)^2}\left(22\,c_F^2 - \frac{107}{9}\,c_F\,N_c + \frac{2}{9}\,c_F\,N_f\right) \tag{23}$$

$Z_{AV}^{L,\overline{MS}}$ can now be obtained by:

$$Z_{AV}^{L,\overline{MS}} = Z_{AV}^{L,RI'} / (C_V\,Z_5) \tag{24}$$

where Z_5 stands for Z_5^s or Z_5^{ns} (Eqs. (22-23)), for the singlet or nonsinglet cases, respectively.

Similarly, one can convert the RI' renormalized Green's functions, $G_\Gamma^{RI'}$, to their $\overline{MS}$ counterparts, through:

$$\frac{G_V^{RI'}}{G_V^{\overline{MS}}} = C_\psi\,C_V \quad,\quad \frac{G_{AV}^{RI'}}{G_{AV}^{\overline{MS}}} = C_\psi\,C_V\,Z_5 \quad,\quad \frac{G_T^{RI'}}{G_T^{\overline{MS}}} = C_\psi\,C_T \tag{25}$$

(In Eqs.(24-25) it is understood that powers of $g_{RI'}$, $\alpha_{RI'}$, implicit in RI' quantities, must also be converted to $g_{\overline{MS}}$, $\alpha_{\overline{MS}}$, respectively, using Eqs.(5-6)). Note that the combination $C_V\,Z_5$ appearing above yields the value of $C_{AV} \equiv Z_{AV}^{DR,RI'}/Z_{AV}^{DR,\overline{MS}} = C_V\,Z_5$.

III. COMPUTATION AND RESULTS

The Feynman diagrams contributing to the bare Green's functions for the vector, axial-vector and tensor operators, $\Sigma^L_{V,AV,T}(q, a_{\text{\tiny L}})$, at 1- and 2-loop level, are shown in Figs. 1 and 2, respectively. For flavor singlet bilinears, there are 4 extra diagrams, shown in Fig. 3, which contain the operator insertion inside a closed fermion loop. These diagrams give a nonzero contribution only in the axial-vector case.

The evaluation and algebraic manipulation of Feynman diagrams, leading to a code for numerical loop integration, is performed automatically using our software for Lattice Perturbation Theory, written in Mathematica.

The most laborious aspect of the procedure is the extraction of the dependence on the external momentum q. This is a delicate task at two loops; for this purpose, we cast algebraic expressions (typically involving thousands of summands) into terms which can be naively Taylor expanded in q to the required order, plus a smaller set of terms containing superficial divergences and/or subdivergences. The latter can be evaluated by an extension of the method of Ref. [33] to 2 loops; this entails analytical continuation to $D > 4$ dimensions, and splitting each expression into a UV-finite part (which can thus be calculated in the continuum, using the methods of Ref. [34]), and a part which is polynomial in q. A primitive set of divergent lattice integrals involving gluon propagators, which can be obtained in this manner, can be found in Ref. [35]. Due to the presence of at least one free Lorentz index in the definition of the operators (for the case of the tensor bilinear there are two such indices), it is possible to end up dealing with superficially divergent integrals with two, three or even four free Lorentz indices. In Appendix B, we provide a brief description of the manipulations performed to resolve such terms, based on the method described above.

Some of the diagrams contributing to $\Sigma^L_{V,AV,T}(qa_{\text{\tiny L}})$ are infrared divergent when considered separately, and thus must be grouped together in order to give finite results. Such groups
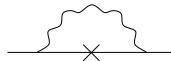
FIG. 1: One-loop diagram contributing to Z_V, Z_{AV} and Z_T. A wavy (solid) line represents gluons (fermions). A cross denotes the Dirac matrices γ_μ (vector), $\gamma_5\gamma_\mu$ (axial vector) and $\gamma_5\sigma_{\mu\nu}$ (tensor).
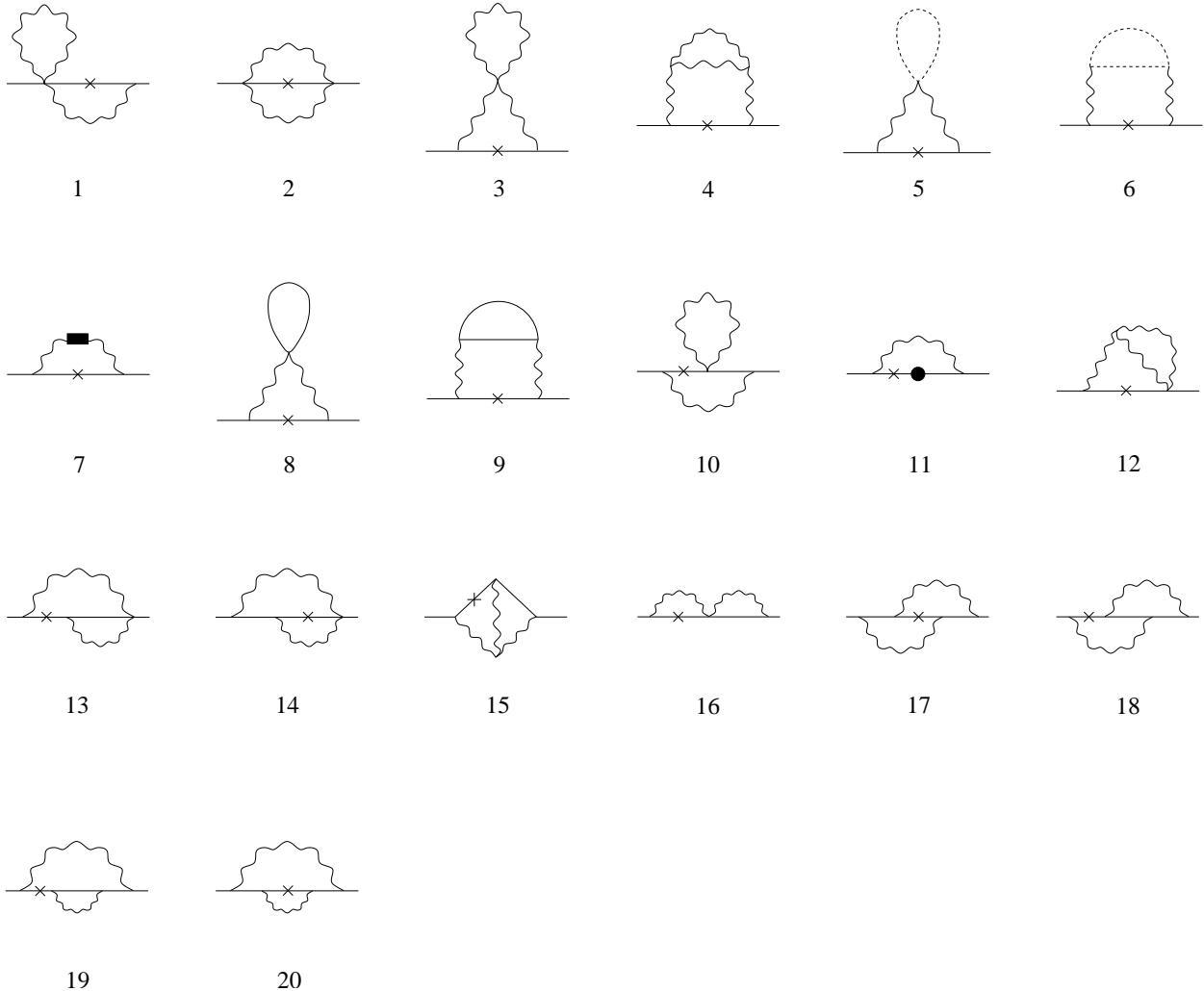
FIG. 2: Two-loop diagrams contributing to Z_V, Z_{AV} and Z_T. Wavy (solid, dotted) lines represent gluons (fermions, ghosts). A solid box denotes a vertex from the measure part of the action; a solid circle is a mass counterterm; crosses denote the matrices γ_μ (vector), $\gamma_5\gamma_\mu$ (axial-vector) and $\gamma_5\sigma_{\mu\nu}$ (tensor).
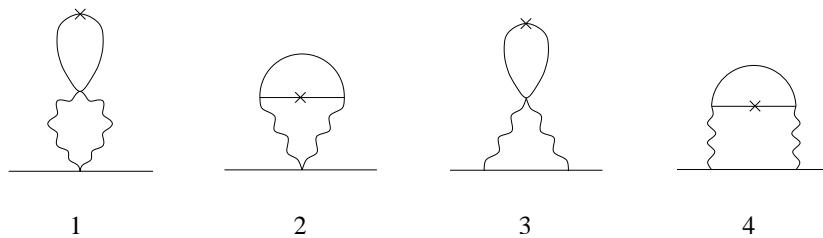

FIG. 3: Extra two-loop diagrams contributing to $Z_{AV,singlet}$. A cross denotes an insertion of a flavor singlet operator. Wavy (solid) lines represent gluons (fermions).

are formed by diagrams (3-7), (8-9), (10-11,19) in Fig. 2 and diagrams (1-2), (3-4) in Fig. 3.

In Figs. 1 to 3, "mirror" diagrams (those in which the direction of the external fermion line is reversed) should also be included. In most cases, these coincide trivially with the original diagrams; even in the remaining cases, they can be seen to give equal contribution, by invariance under charge conjugation.

As mentioned before, all calculations should be performed at vanishing renormalized mass; this can be achieved by working with massless fermion propagators, provided an appropriate fermion mass counterterm is introduced (diagram 11 in Fig. 2).

All two-loop diagrams have been calculated in the bare Feynman gauge ($\alpha_\circ = 1$). One-loop diagrams have been calculated for generic values of $\alpha_\circ$; this allows us to convert our two-loop results to the renormalized Feynman gauge ($\alpha_{RI'} = 1$ or $\alpha_{\overline{MS}} = 1$). After performing the calculation for the cases of the vector and axial-vector operator, we see that one-loop expressions for the renormalization functions do not depend on the gauge parameter. Especially for the case of the vector operator, having in mind Eqs. (5-6) and Eq. (16), this fact causes the lattice results in the RI' and in the $\overline{MS}$ scheme to coincide.

Numerical loop integration was carried out by our "integrator" program, a *metacode* written in Mathematica, for converting lengthy integrands into efficient Fortran code. Two-loop numerical integrals were evaluated as sums over finite lattices, of size up to $L = 40$; the results were then extrapolated to $L \to \infty$. Extrapolation is the only source of systematic error; this error can be estimated quite accurately (see, e.g. Ref. [36]), given that L-dependence of results can only span a restricted set of functional forms.

A. One-loop results

1-loop results for $Z_\Gamma^{L,RI'}$ are presented below in a generic gauge. As it turns out, only the tensor renormalization function depends on the gauge parameter, while for all other operators, one-loop expressions that emerge are gauge independent. The errors appearing in the expression for $Z_T^{L,RI'}$, result from the $L \to \infty$ extrapolation.

$$Z_T^{L,RI'} = 1 + \frac{g_\circ^2}{16\pi^2} c_F \left[-\ln(a_{\mathrm{L}}^2 \bar{\mu}^2) + \alpha_\circ - 17.018079209(7) \right.$$
$$\left. + 3.91333261(4) c_{\mathrm{SW}} + 1.972295300(5) c_{\mathrm{SW}}^2 \right] \tag{26}$$

The corresponding expressions for $Z_V^{L,RI'}$, $Z_{AV}^{L,RI'}$ can be read off from Eqs. (30-31) below. In all cases, one-loop results in the $\overline{MS}$ scheme ($Z_V^{L,\overline{MS}}$, $Z_{AV}^{L,\overline{MS}}$, $Z_T^{L,\overline{MS}}$) present no dependence on the gauge parameter.

B.   Two-loop results

In order to derive the expressions for the bare Green's functions $\Sigma_{V,AV,T}^L$, one must evaluate all Feynman diagrams presented in Figs. 1-3. The extraction of $Z_V^{L,Y}$, $Z_{AV}^{L,Y}$ and $Z_T^{L,Y}$ is then straightforward via Eqs. (11-13) (for $Y = RI'$), and via Eqs. (15-17, 24) (for $Y = \overline{MS}$). To this end, we need the following one-loop expression for $Z_A^{L,Y}$ (note that $Z_\alpha = 1$ to this order):

$$
\begin{aligned}
Z_A^{L,RI'} &= Z_A^{L,\overline{MS}} + \mathcal{O}\left(g_\text{o}^4\right) \\
&= 1 + \frac{g_\text{o}^2}{16\pi^2}\Bigg[\ln\left(a_\text{L}^2\bar{\mu}^2\right)\left(\frac{2}{3}N_f - \frac{5}{3}N_c\right) \\
&\quad + N_f\left(-2.168501047(1) + 0.7969452308(4)\,c_\text{SW} - 4.7126914428(1)\,c_\text{SW}^2\right) \\
&\quad + 39.47841760436(1)\,c_F + 1.94017130069(1)\,N_c\Bigg] + \mathcal{O}\left(g_\text{o}^4\right)
\end{aligned}
\tag{27}
$$

To express our results in terms of the renormalized coupling constant, we also need the one-loop expression for $Z_g^{L,Y}$:

$$
\begin{aligned}
Z_g^{L,RI'} &= Z_g^{L,\overline{MS}} + \mathcal{O}\left(g_\text{o}^4\right) \\
&= 1 + \frac{g_\text{o}^2}{16\pi^2}\Bigg[\ln\left(a_\text{L}^2\bar{\mu}^2\right)\left(-\frac{1}{3}N_f + \frac{11}{6}N_c\right) \\
&\quad + N_f\left(0.5286949677(5) - 0.3984726154(2)\,c_\text{SW} + 2.35634572140(7)\,c_\text{SW}^2\right) \\
&\quad - 19.73920880218(1)\,c_F - 3.54958342046(1)\,N_c\Bigg] + \mathcal{O}\left(g_\text{o}^4\right)
\end{aligned}
\tag{28}
$$

Eqs. (27, 28) are in agreement with older references (see, e.g., Ref. [37]).

A final necessary ingredient is the two-loop expression for $Z_\psi^{L,RI'}$, as required by Eqs.(11-13); this was calculated in Ref. [1], in the renormalized Feynman gauge $\alpha_{RI'} = 1$, and is included here for completeness:

$$Z_\psi^{L,RI'} = 1 + \frac{g_\circ^2}{16\pi^2} c_F \left[\ln(a_{\rm L}^2 \bar\mu^2) + 11.852404288(5) - 2.248868528(3)\, c_{\rm SW} - 1.397267102(5)\, c_{\rm SW}^2 \right]$$

$$+ \frac{g_\circ^4}{(16\pi^2)^2} c_F \left[\ln^2(a_{\rm L}^2 \bar\mu^2) \left(\frac{1}{2} c_F + \frac{2}{3} N_f - \frac{8}{3} N_c \right) \right.$$

$$+ \ln(a_{\rm L}^2 \bar\mu^2) \Big(-6.36317446(8)\, N_f + 0.79694523(2)\, N_f\, c_{\rm SW}$$

$$-4.712691443(4)\, N_f\, c_{\rm SW}^2$$

$$+49.83082185(5)\, c_F - 2.24886861(7)\, c_F\, c_{\rm SW}$$

$$-1.39726705(1)\, c_F\, c_{\rm SW}^2 + 29.03029398(4)\, N_c \Big)$$

$$+ N_f \Big(-7.838(2) + 1.153(1)\, c_{\rm SW} + 3.202(3)\, c_{\rm SW}^2$$

$$+6.2477(6)\, c_{\rm SW}^3 + 4.0232(6)\, c_{\rm SW}^4 \Big)$$

$$+ c_F \Big(505.39(1) - 58.210(9)\, c_{\rm SW} + 20.405(5)\, c_{\rm SW}^2$$

$$+18.8431(8)\, c_{\rm SW}^3 + 4.2793(2)\, c_{\rm SW}^4 \Big)$$

$$+ N_c \Big(-20.59(1) - 3.190(5)\, c_{\rm SW} - 23.107(6)\, c_{\rm SW}^2$$

$$\left. -5.7234(5)\, c_{\rm SW}^3 - 0.7938(1)\, c_{\rm SW}^4 \Big) \right] \tag{29}$$

We present below $Z_V^{L,RI'}$, $Z_{AV}^{L,RI'}$ and $Z_T^{L,RI'}$ to two loops in the renormalized Feynman gauge $\alpha_{RI'} = 1$; we also present the $\overline{MS}$ analogues $Z_{AV}^{L,\overline{MS}}$ and $Z_T^{L,\overline{MS}}$ in the gauge $\alpha_{\overline{MS}} = 1$ (as already mentioned, $Z_V^{L,\overline{MS}} = Z_V^{L,RI'}$). The bare Green's functions are relegated to Appendix C, where a *per diagram* breakdown of the results is provided. It is a straightforward exercise to recover the total bare Green's functions from the corresponding Z's and the renormalized Green's functions.

$$Z_V^{L,RI'} = 1 + \frac{g_\circ^2}{16\pi^2} c_F \left[-20.617798655(6) + 4.745564682(3)\, c_{\rm SW} + 0.543168028(5)\, c_{\rm SW}^2 \right]$$

$$+ \frac{g_\circ^4}{(16\pi^2)^2} c_F \left[N_f \Big(25.610(3) - 11.058(1)\, c_{\rm SW} + 33.937(3)\, c_{\rm SW}^2 \right.$$

$$-13.5286(6)\, c_{\rm SW}^3 - 1.2914(6)\, c_{\rm SW}^4 \Big)$$

$$+ c_F \Big(-539.78(1) - 223.57(2)\, c_{\rm SW} - 104.116(5)\, c_{\rm SW}^2$$

$$-32.2623(8)\, c_{\rm SW}^3 + 4.5575(3)\, c_{\rm SW}^4 \Big)$$

$$+ N_c \Big(-51.59(1) + 18.543(5)\, c_{\rm SW} + 20.960(6)\, c_{\rm SW}^2$$

$$\left. +2.5121(5)\, c_{\rm SW}^3 + 0.1765(1)\, c_{\rm SW}^4 \Big) \right] \tag{30}$$

$$Z_{AV}^{L,RI'} = 1 \; + \; \frac{g_\circ^2}{16\pi^2} \, c_F \Big[-15.796283066(5) - 0.247827627(3) \, c_{\mathrm{SW}} + 2.251366176(5) \, c_{\mathrm{SW}}^2 \Big]$$
$$+ \; \frac{g_\circ^4}{(16\pi^2)^2} \, c_F \Big[N_f \Big(18.497(3) - 1.285(1) \, c_{\mathrm{SW}} + 19.071(3) \, c_{\mathrm{SW}}^2$$
$$+ 1.0333(6) \, c_{\mathrm{SW}}^3 - 6.7549(6) \, c_{\mathrm{SW}}^4 \Big)$$
$$+ c_F \Big(-184.01(1) - 389.86(1) \, c_{\mathrm{SW}} - 166.738(6) \, c_{\mathrm{SW}}^2$$
$$+ 7.894(1) \, c_{\mathrm{SW}}^3 + 4.3201(3) \, c_{\mathrm{SW}}^4 \Big)$$
$$+ N_c \Big(-21.62(1) - 33.652(5) \, c_{\mathrm{SW}} + 26.636(6) \, c_{\mathrm{SW}}^2$$
$$+ 10.2186(5) \, c_{\mathrm{SW}}^3 + 1.4893(1) \, c_{\mathrm{SW}}^4 \Big) \Big] \tag{31}$$

$$Z_{AV}^{L,\overline{MS}} = 1 \; + \; \frac{g_\circ^2}{16\pi^2} \, c_F \Big[-11.796283066(5) - 0.247827627(3) \, c_{\mathrm{SW}} + 2.251366176(5) \, c_{\mathrm{SW}}^2 \Big]$$
$$+ \; \frac{g_\circ^4}{(16\pi^2)^2} \, c_F \Big[\ln(a_{\mathrm{L}}^2 \bar{\mu}^2) \Big(\frac{8}{3} \, N_f - \frac{44}{3} \, N_c \Big)$$
$$+ N_f \Big(14.045(3) + 1.903(1) \, c_{\mathrm{SW}} + 0.220(3) \, c_{\mathrm{SW}}^2$$
$$+ 1.0333(6) \, c_{\mathrm{SW}}^3 - 6.7549(6) \, c_{\mathrm{SW}}^4 \Big)$$
$$+ c_F \Big(-95.28(1) - 390.85(1) \, c_{\mathrm{SW}} - 157.733(6) \, c_{\mathrm{SW}}^2$$
$$+ 7.894(1) \, c_{\mathrm{SW}}^3 + 4.3201(3) \, c_{\mathrm{SW}}^4 \Big)$$
$$+ N_c \Big(18.67(1) - 33.652(5) \, c_{\mathrm{SW}} + 26.636(6) \, c_{\mathrm{SW}}^2$$
$$+ 10.2186(5) \, c_{\mathrm{SW}}^3 + 1.4893(1) \, c_{\mathrm{SW}}^4 \Big) \Big] \tag{32}$$

$$Z_T^{L,RI'} = 1 \; + \; \frac{g_\circ^2}{16\pi^2} \, c_F \Big[-\ln(a_{\mathrm{L}}^2 \bar{\mu}^2) - 16.018079209(7)$$
$$+ 3.91333261(4) \, c_{\mathrm{SW}} + 1.972295300(5) \, c_{\mathrm{SW}}^2 \Big]$$
$$+ \; \frac{g_\circ^4}{(16\pi^2)^2} \, c_F \Big[\ln^2(a_{\mathrm{L}}^2 \bar{\mu}^2) \Big(\frac{1}{2} c_F - \frac{1}{3} N_f - \frac{11}{6} N_c \Big)$$
$$+ \ln(a_{\mathrm{L}}^2 \bar{\mu}^2) \Big(3.1685002(6) \, N_f - 0.79694524(6) \, N_f \, c_{\mathrm{SW}}$$
$$+ 4.71269143(3) \, N_f \, c_{\mathrm{SW}}^2$$
$$- 13.96033835(7) \, c_F - 3.9133325(1) \, c_F \, c_{\mathrm{SW}}$$
$$- 1.97229535(2) \, c_F \, c_{\mathrm{SW}}^2 - 25.04361149(6) \, N_c \Big)$$
$$+ N_f \Big(16.923(6) - 8.399(2) \, c_{\mathrm{SW}} + 18.711(3) \, c_{\mathrm{SW}}^2$$

15

$$-10.8351(8)\, c_{\mathrm{SW}}^3 - 5.1253(6)\, c_{\mathrm{SW}}^4\Big)$$

$$+c_F\Big(-868.0(1) + 551.6(2)\, c_{\mathrm{SW}} + 63.9(1)\, c_{\mathrm{SW}}^2$$

$$-79.49(1)\, c_{\mathrm{SW}}^3 - 12.586(1)\, c_{\mathrm{SW}}^4\Big)$$

$$+N_c\Big(-15.76(8) + 27.6(1)\, c_{\mathrm{SW}} + 38.2(1)\, c_{\mathrm{SW}}^2$$

$$+7.021(8)\, c_{\mathrm{SW}}^3 + 1.6653(9)\, c_{\mathrm{SW}}^4\Big)\Bigg] \tag{33}$$

$$Z_T^{L,\overline{MS}} = 1 + \frac{g_\circ^2}{16\pi^2}\, c_F\Big[-\ln(a_{\mathrm{L}}^2\bar\mu^2) - 17.018079209(7)$$

$$+3.91333261(4)\, c_{\mathrm{SW}} + 1.972295300(5)\, c_{\mathrm{SW}}^2\Big]$$

$$+ \frac{g_\circ^4}{(16\pi^2)^2}\, c_F\Bigg[\ln^2(a_{\mathrm{L}}^2\bar\mu^2)\Big(-\frac{1}{3}\,N_f + \frac{1}{2}\,c_F + \frac{11}{6}\,N_c\Big)$$

$$+ \ln(a_{\mathrm{L}}^2\bar\mu^2)\Big(2.5018336(6)\, N_f - 0.79694524(6)\, N_f\, c_{\mathrm{SW}}$$

$$+4.71269143(3)\, N_f\, c_{\mathrm{SW}}^2$$

$$-12.96033835(7)\, c_F - 3.9133325(1)\, c_F\, c_{\mathrm{SW}}$$

$$-1.97229535(2)\, c_F\, c_{\mathrm{SW}}^2 - 21.37694482(6)\, N_c\Big)$$

$$+N_f\Big(21.989(6) - 9.196(2)\, c_{\mathrm{SW}} + 23.424(3)\, c_{\mathrm{SW}}^2$$

$$-10.8351(8)\, c_{\mathrm{SW}}^3 - 5.1253(6)\, c_{\mathrm{SW}}^4\Big)$$

$$+c_F\Big(-893.2(1) + 547.7(2)\, c_{\mathrm{SW}} + 61.9(1)\, c_{\mathrm{SW}}^2$$

$$-79.49(1)\, c_{\mathrm{SW}}^3 - 12.586(1)\, c_{\mathrm{SW}}^4\Big)$$

$$+N_c\Big(-41.44(8) + 27.6(1)\, c_{\mathrm{SW}} + 38.2(1)\, c_{\mathrm{SW}}^2$$

$$+7.021(8)\, c_{\mathrm{SW}}^3 + 1.6653(9)\, c_{\mathrm{SW}}^4\Big)\Bigg] \tag{34}$$

All expressions reported thus far for Z_V, Z_{AV} and Z_T refer to flavor nonsinglet operators. In the case of Z_V and Z_T, all diagrams of Fig. 3 vanish, so that singlet and nonsinglet results coincide, just as in dimensional regularization. For Z_{AV} on the other hand, the above diagrams give an additional contribution:

$$Z_{AV,\,\mathrm{singlet}}^{L,RI'} = Z_{AV}^{L,RI'} + \frac{g_\circ^4}{(16\pi^2)^2}\, c_F N_f\Big(-6\,\ln(a_{\mathrm{L}}^2\bar\mu^2) - 2.0491(5) + 15.0315(6)\, c_{\mathrm{SW}}$$

$$+5.0090(2)\, c_{\mathrm{SW}}^2 - 2.11016(5)\, c_{\mathrm{SW}}^3 - 0.04329(2)\, c_{\mathrm{SW}}^4\Big) \tag{35}$$

The same extra contribution applies also to the $\overline{MS}$ scheme.

For the sake of completeness, and as an additional check on our results, we compute the renormalized Green's functions (for *vanishing* renormalized mass). Since the bare Green's

functions have two contributions of different structure (as defined in Eq. (10), see also Eq. (20)), we derive the renormalized expressions for these contributions separately:

$$G_V^{(i)\,RI'}(q) \equiv Z_\psi^{L,RI'}\, Z_V^{L,RI'}\, \Sigma_V^{(i),L} \tag{36}$$

$$G_{AV}^{(i)\,RI'}(q) \equiv Z_\psi^{L,RI'}\, Z_{AV}^{L,RI'}\, \Sigma_{AV}^{(i),L} \tag{37}$$

$$G_T^{(i)\,RI'}(q) \equiv Z_\psi^{L,RI'}\, Z_T^{L,RI'}\, \Sigma_T^{(i),L} \tag{38}$$

where $i = 1, 2$. Similarly for $\overline{MS}$, taking into account Eq. (25).

Since these functions are regularization independent, they can be calculated also using, e.g., dimensional regularization. We have computed $G_V^{(i)}$, $G_{AV}^{(i)}$ and $G_T^{(i)}$ in both ways: either starting from our Eqs.(26-34) or using renormalization functions from dimensional regularization [2]. In all cases the two ways are in complete agreement. We obtain:

$$G_V^{(1)\,RI'}(q) = 1 + \frac{g_{RI'}^2}{16\pi^2}\, c_F \ln(\bar{\mu}^2/q^2)$$
$$+ \frac{g_{RI'}^4}{(16\pi^2)^2}\, c_F \left[\ln^2(\bar{\mu}^2/q^2) \left(\frac{1}{2}\, c_F + N_c \right) \right.$$
$$\left. + \ln(\bar{\mu}^2/q^2) \left(-\frac{19}{9}\, N_f - \frac{3}{2}\, c_F + \frac{251}{18}\, N_c \right) \right] \tag{39}$$

$$G_V^{(2)\,RI'}(q) = \frac{g_{RI'}^2}{16\pi^2}\, c_F \left(-2 \ln(\bar{\mu}^2/q^2) \right)$$
$$+ \frac{g_{RI'}^4}{(16\pi^2)^2}\, c_F \left[\ln(\bar{\mu}^2/q^2)\, (-2\, c_F - 4\, N_c) + \frac{38}{9}\, N_f + 3\, c_F - \frac{251}{9}\, N_c \right] \tag{40}$$

The vector renormalized Green's function in the RI' scheme coincides with the corresponding axial-vector expression, and thus Eqs.(39-40) also hold for the axial-vector case: $G_{AV}^{(1)}(q) = G_V^{(1)}(q)$, $G_{AV}^{(2)}(q) = G_V^{(2)}(q)$. Of course, even though the $\overline{MS}$ expression for the vector renormalization function, $Z_V^{L,\overline{MS}}$, coincides with the RI' expression, that is not the case for the renormalized $\overline{MS}$ Green's function, due to C_ψ appearing in Eq. (25). This factor results in the following quantities:

$$G_V^{(1)\,\overline{MS}}(q) = 1 + \frac{g_{\overline{MS}}^2}{16\pi^2}\, c_F \left(\ln(\bar{\mu}^2/q^2) + 1 \right)$$
$$+ \frac{g_{\overline{MS}}^4}{(16\pi^2)^2}\, c_F \left[\ln^2(\bar{\mu}^2/q^2) \left(\frac{1}{2}\, c_F + N_c \right) \right.$$
$$+ \ln(\bar{\mu}^2/q^2) \left(-\frac{19}{9}\, N_f - \frac{1}{2}\, c_F + \frac{251}{18}\, N_c \right)$$
$$\left. + \left(-\frac{7}{4}\, N_f - \frac{5}{8}\, c_F + \left(\frac{143}{8} - 6\zeta(3) \right) N_c \right) \right] \tag{41}$$

17

$$G_V^{(2)\,\overline{MS}}(q) = -\frac{g_{\overline{MS}}^2}{16\pi^2}\,2\,c_F$$
$$+\ \frac{g_{\overline{MS}}^4}{(16\pi^2)^2}\,c_F\left[\ln(\bar\mu^2/q^2)\,(-2\,c_F - 4\,N_c) + \frac{38}{9}\,N_f + c_F - \frac{251}{9}\,N_c\right] \quad (42)$$

Furthermore, the axial-vector renormalized 2-point functions in the $\overline{MS}$ scheme differ from Eqs. (41-42), due to the finite conversion factor Z_5^{ns}; they read:

$$G_{AV}^{(1)\,\overline{MS}}(q) = 1\ +\ \frac{g_{\overline{MS}}^2}{16\pi^2}\,c_F\left(\ln(\bar\mu^2/q^2) + 5\right)$$
$$+\ \frac{g_{\overline{MS}}^4}{(16\pi^2)^2}\,c_F\left[\ln^2(\bar\mu^2/q^2)\left(\frac{1}{2}\,c_F + N_c\right)\right.$$
$$+\ln(\bar\mu^2/q^2)\left(-\frac{19}{9}\,N_f + \frac{7}{2}\,c_F + \frac{251}{18}\,N_c\right)$$
$$\left.+\left(-\frac{71}{36}\,N_f - \frac{21}{8}\,c_F + \left(\frac{2143}{72} - 6\zeta(3)\right)N_c\right)\right] \quad (43)$$

$$G_{AV}^{(2)\,\overline{MS}}(q) = -\frac{g_{\overline{MS}}^2}{16\pi^2}\,2\,c_F$$
$$+\ \frac{g_{\overline{MS}}^4}{(16\pi^2)^2}\,c_F\left[\ln(\bar\mu^2/q^2)\,(-2\,c_F - 4\,N_c) + \frac{38}{9}\,N_f - 7\,c_F - \frac{251}{9}\,N_c\right] \quad (44)$$

If one considers the singlet axial-vector current, then there exists an extra contribution to the expressions above:

$$G_{AV,\,\text{singlet}}^{(1),\,\overline{MS}}(q) = G_{AV}^{(1)\,\overline{MS}}(q) + \frac{g_{\overline{MS}}^4}{(16\pi^2)^2}\left(-6\,\ln(\bar\mu^2/q^2)\,c_F N_f - \frac{3}{2}\,c_F N_f\right) \quad (45)$$

$$G_{AV,\,\text{singlet}}^{(2),\,\overline{MS}}(q) = G_{AV}^{(2)\,\overline{MS}}(q) + \frac{g_{\overline{MS}}^4}{(16\pi^2)^2}\left(-4\,c_F N_f\right) \quad (46)$$

For the RI' scheme, similar relations hold, the only difference being the absence of the factors Z_5^s, Z_5^{ns}; we obtain:

$$G_{AV,\,\text{singlet}}^{(1),\,RI'}(q) = G_{AV}^{(1)\,RI'}(q) + \frac{g_{RI'}^4}{(16\pi^2)^2}\left(-6\,\ln(\bar\mu^2/q^2)\,c_F N_f\right) \quad (47)$$

$$G_{AV,\,\text{singlet}}^{(2),\,RI'}(q) = G_{AV}^{(2)\,RI'}(q) + \frac{g_{RI'}^4}{(16\pi^2)^2}\left(-4\,c_F N_f\right) \quad (48)$$

Finally, for the tensor renormalized Green's function, we obtain:

$$G_T^{(1)\,RI'}(q) = 1\ +\ \frac{g_{RI'}^4}{(16\pi^2)^2}\,c_F\left[\ln^2(\bar\mu^2/q^2)\left(\frac{1}{3}\,N_f - \frac{5}{6}\,N_c\right)\right.$$
$$\left.+\ln(\bar\mu^2/q^2)\left(-\frac{2}{3}\,N_f + 8\,c_F - \frac{7}{3}\,N_c\right)\right] \quad (49)$$

Just as was expected from dimensional regularization, $G_T^{(2)\,RI'}(q) = 0$. The corresponding quantity in the $\overline{MS}$ scheme reads:

$$
\begin{aligned}
G_T^{(1)\,\overline{MS}}(q) = 1 \; + \; \frac{g_{\overline{MS}}^4}{(16\pi^2)^2}\, c_F &\left[\ln^2(\bar{\mu}^2/q^2) \left(\frac{1}{3}\, N_f - \frac{5}{6}\, N_c \right) \right. \\
&+ \ln(\bar{\mu}^2/q^2) \left(-\frac{2}{3}\, N_f + 8\, c_F - \frac{7}{3}\, N_c \right) \\
&\left. + \frac{31}{27}\, N_f + \left(\frac{62}{3} - 20\, \zeta(3) \right) c_F + \left(-\frac{761}{54} + 8\, \zeta(3) \right) \right] \quad (50)
\end{aligned}
$$

In Figs. 4, (5,6), (7,8) we plot $Z_V^{L,RI'}$, $(Z_{AV}^{L,RI'}, Z_{AV}^{L,\overline{MS}})$ and $(Z_T^{L,RI'}, Z_T^{L,\overline{MS}})$, respectively, as a function of c_{SW}. Values of the clover parameter used in simulations lie within the typical range $0 \leq c_{\mathrm{SW}} \lesssim 2$. For definiteness, we have set $N_c = 3$, $\bar{\mu} = 1/a_{\mathrm{L}}$ and $\beta_{\mathrm{o}} \equiv 2N_c/g_{\mathrm{o}}^2 = 6.0$. Our results up to two loops for each Z are shown for both $N_f = 0$ and $N_f = 2$, and compared to the corresponding one-loop results. Furthermore, in the axial-vector case, we also present the two-loop result for the flavor singlet operator, for $N_f = 2$.

In Fig. 9 we present, on the same plot, the values of $Z_V^{L,RI'}$, $Z_{AV}^{L,RI'}$, $Z_{AV,\,singlet}^{L,RI'}$ and $Z_T^{L,RI'}$ up to 2 loops, versus c_{SW}. We have chosen $N_c = 3$, $\bar{\mu} = 1/a_{\mathrm{L}}$, $N_f = 2$ and $\beta_{\mathrm{o}} = 5.3$. The corresponding results in the $\overline{MS}$ scheme are plotted in Fig. 10.

IV. DISCUSSION

In this paper we have reported results regarding the Vector, Axial-Vector and Tensor fermion bilinear operators. This work, along with a previously published paper [1] regarding the Scalar and Pseudoscalar operators, provide a complete two loop calculation for the renormalization functions for local fermion bilinears, considering both the singlet and nonsinglet cases. The two-loop wave function renormalization constant, Z_ψ, which is a prerequisite for our calculation, was presented in Ref. [1] (the reader should also refer to this paper for any necessary notation not included in the present sequel paper).

It is clear from Figs. 4 to 8 that the two-loop renormalization functions differ significantly from 1-loop values; this difference must then be properly taken into account in reducing systematic error in MC simulations. At the same time, 2-loop contributions are typically smaller than 1-loop contributions, especially for $c_{SW} \lesssim 1$, indicating that the (asymptotic) perturbative series are under control.

The results are presented as a function of the clover parameter, where the values of c_{SW} lie within the standard range $0 \le c_{SW} \le 2$. Optimal values for c_{SW}, which have been estimated both non-perturbatively [38] and perturbatively (to 1-loop) [25], lie within this range. A breakdown of our results on a *per diagram* basis is presented in Appendix C, for completeness.

As already mentioned, we take into account both singlet and nonsinglet operators. After evaluating all Feynman diagrams involved, we found that, for the Vector and Tensor operators, singlet renormalization functions coincide with nonsinglet ones. On the other hand, the Axial-Vector operator receives an additional contribution in the flavor singlet case.

The numerical integrations over loop momenta were executed on a Pentium IV cluster; they required the equivalent of 60 months on a single CPU.

A possible extension to the present calculation is the renormalization of more extended operators, with the same continuum limit as we have considered here. A standard basis of higher dimension operators, with the same quantum numbers as the local bilinears which we have considered, can be found e.g. in Ref. [5]. Such operators are frequently used to reduce $\mathcal{O}(a_{\rm L})$ effects. A number of additional Feynman diagrams must be introduced, since the vertices coming from these operators may also contain gluon lines. However, the additional integrals resulting after the contractions will be free of superficial divergences,

leading to a less cumbersome computation, despite an increase in the size of the integrals. Further directions regard higher dimensional operators, such as $\bar{\Psi}\, D^\mu \cdots D^\nu\, \Gamma\Psi$, which enter structure function calculations, and 4-fermion operators.

Finally, our computation can be easily extended to improved lattice actions. With regard to improved fermion actions, such as those containing twisted mass terms [39] or Österwalder-Seiler terms [40], our results remain unchanged, since they pertain to mass-independent schemes. Improving the gluon action, on the other hand, is more CPU consuming, but conceptually straightforward: Splitting (in iterative fashion) the Symanzik propagator into a Wilson gluon propagator plus the remainder, leads to the same bare Green's functions as the ones presented in this paper, with the addition of superficially convergent terms, which can be more easily manipulated. Based on our experience with other similar calculations, the algebraic expressions for the integrands will grow roughly by a factor of 5; furthermore, the gluon propagator must now be inverted numerically for each value of the momentum, leading to an additional factor of $\lesssim 2$ in CPU time. Finally, if one wishes to employ more than one set of values for the Symanzik coefficients, CPU time for numerical integration will increase almost proportionately.

APPENDIX A: FERMIONS IN AN ARBITRARY REPRESENTATION

The results presented up to this point regarded renormalization constants of various fermion bilinear operators constructed with fermions in the fundamental representation of the gauge group. Our results were expressed in terms of the clover parameter, c_{SW}, the number of fermions, N_f, the number of colors, N_c, and the quadratic Casimir operator in the fundamental representation, c_F.

Recently there has been interest in theories with fermions in other representations; some preliminary non-perturbative calculations have also appeared (see e.g. [41], [42]). In this Appendix we describe the conventions we use in our work, regarding the generators of the algebra, and we then express our findings in an arbitrary representation.

Our results for Z_V, Z_{AV}, Z_T, Eqs.(30, 31, 33), can be easily generalized to an action with Wilson/clover fermions in an arbitrary representation R, of dimensionality d_R.

In this case, the gluon part of the action remains the same, while all link variables appearing in the fermion part of the action assume the form:

$$U_{x,\,x+\mu} = \exp(i\,g_0\,A_\mu^a(x)\,T^a) \quad \longrightarrow \quad U_{x,\,x+\mu} = \exp(i\,g_0\,A_\mu^a(x)\,T_R^a) \tag{A1}$$

Using standard notation and conventions, the generators T^a in the fundamental representation satisfy:

$$[T^a, T^b] = i\,f^{abc}\,T^c, \quad \sum_a T^a T^a \equiv \mathbb{1} \cdot c_F = \mathbb{1} \cdot \frac{N_c^2 - 1}{2N_c}, \quad \mathrm{tr}(T^a T^b) \equiv \delta^{ab}\,t_F = \delta^{ab}\,\frac{1}{2} \tag{A2}$$

In the representation R we have:

$$[T_R^a, T_R^b] = i\,f^{abc}\,T_R^c, \quad \sum_a T_R^a T_R^a \equiv \mathbb{1} \cdot c_R, \quad \mathrm{tr}(T_R^a T_R^b) \equiv \delta^{ab}\,t_R \tag{A3}$$

where: $t_R = (d_R\,c_R)/(N_c^2 - 1)$.

For the 1-loop quantities, Eqs. (27, 28), converting to the representation R is a straightforward substitution:

$$N_f \longrightarrow N_f \cdot (t_R/t_F) = N_f \cdot (2\,t_R) \tag{A4}$$

and, in addition, for Eq. (26):

$$c_F \longrightarrow c_R \tag{A5}$$

Aside from these changes, all algebraic expressions (and the numerical coefficients resulting from loop integrations) remain the same.

A similar reasoning applies to the 2-loop quantities in Eqs. (30, 31, 33): For most diagrams, once their value is expressed as a linear combination of c_F^2, $c_F N_c$ and $c_F N_f$, it suffices to apply substitutions (A4) and (A5). The only exceptions are diagrams containing a gluon tadpole [diagram 3 of Fig. 2; 1-loop diagrams, when expressed in terms of $a_{RI'}$, $\alpha_{RI'}$ by means of Z_g, Z_A]: In these cases, only one power of c_F should be changed to c_R; a possible additional power of c_F originates from the gluon tadpole and should stay as is. This peculiarity implies that, in order to perform the substitutions as described above, one must start from the *per diagram* breakdown of 2-loop results. To avoid a lengthy presentation, we apply, instead, substitutions (A4) and (A5) indiscriminately on Eqs. (30, 31, 33); consequently, we must then add a correction term, as follows:

$$
\begin{aligned}
Z_V^{L,RI'}\big|_R = {}& Z_V^{L,RI'}\big|_{c_F \to c_R,\ N_f \to 2N_f t_R} \\
&+ \frac{g_\circ^4}{(16\pi^2)^2}\, c_R\,(c_R - c_F) \cdot [813.9580654(2) - 187.3473843(1)\, c_{\mathrm{SW}} \\
&\qquad\qquad\qquad\qquad\qquad - 21.4434142(2)\, c_{\mathrm{SW}}^2]
\end{aligned}
\tag{A6}
$$

$$
\begin{aligned}
Z_{AV}^{L,RI'}\big|_R = {}& Z_{AV}^{L,RI'}\big|_{c_F \to c_R,\ N_f \to 2N_f t_R} \\
&+ \frac{g_\circ^4}{(16\pi^2)^2}\, c_R\,(c_R - c_F) \cdot [623.6122595(2) + 9.7838425(1)\, c_{\mathrm{SW}} \\
&\qquad\qquad\qquad\qquad\qquad - 88.8803741(2)\, c_{\mathrm{SW}}^2]
\end{aligned}
\tag{A7}
$$

$$
\begin{aligned}
Z_T^{L,RI'}\big|_R = {}& Z_T^{L,RI'}\big|_{c_F \to c_R,\ N_f \to 2N_f t_R} \\
&+ \frac{g_\circ^4}{(16\pi^2)^2}\, c_R\,(c_R - c_F) \cdot [4\pi^2 \ln(a_{\mathrm{L}}^2 \bar{\mu}^2) + 632.3684202(3) \\
&\qquad\qquad\qquad\qquad\qquad - 154.492179(2)\, c_{\mathrm{SW}} - 77.8630975(2)\, c_{\mathrm{SW}}^2]
\end{aligned}
\tag{A8}
$$

Actually, the reader could arrive at these results without knowledge of the per diagram breakdown, by virtue of the following fact: All "exceptional" powers of c_F cancel out of $Z_V^{L,RI'}$, $Z_{AV}^{L,RI'}$, $Z_T^{L,RI'}$, if these are expressed in terms of the renormalized coupling constant $a_{RI'}$. Thus, one may:

- Express Eqs. (30, 31, 33) in terms of $g_{RI'}$ by means of $g_\circ = (Z_g^{L,RI'})\, g_{RI'}$, with $Z_g^{L,RI'}$ in the fundamental representation (Eq. (28))

- Apply substitutions (A4), (A5) throughout

- If desired, reexpress everything in terms of $g_\circ$ (using $(Z_g^{L,RI'})^{-1}$ from Eq. (28), with $N_f \to 2N_f t_R$ and c_F as is)

No correction terms are necessary in this procedure.

APPENDIX B: MANIPULATION OF SUPERFICIALLY DIVERGENT AND SUBDIVERGENT TERMS

In the case of the Scalar and Pseudoscalar bilinears [1] all superficially divergent terms involved at most one free Lorentz index, but when one considers other bilinear operators different structures may arise. For example, in the case of the vector and axial-vector operators, two-index integrals may arise and, of course, when working with the tensor operator three- or even four-index integrals appear during the manipulation of superficially divergent terms. The most laborious aspect of such an evaluation is to extract the explicit dependence of the bare matrix element on the external momentum, by expressing the superficially divergent parts in terms of known primitive divergent integrals.

We will focus on an arbitrary four-index integrand emerging, for example, from a "diamond"-like diagram with a $\Gamma = \gamma_5\,\sigma_{\mu\nu}$ insertion. Taking into account the symmetries of this object, we can deduce all possible tensor structures which may appear, as a linear combination, in the result for the corresponding integral. Such structures are certainly tensors under the hypercubic group, but not necessarily so under the full $SO(4)$ Euclidean rotation group: Terms such as $\delta^{\mu\nu\rho\sigma}$ or $q^4/(q^2)^2$ might be present[1] (q: external momentum), and if so they might spoil the renormalizability and/or the Lorentz invariance of the theory. We must show that in all cases, such terms are absent.

Let us begin by taking as an example an algebraic expression which contains both superficial and sub divergencies; this example serves as a prototype for all the cases we have encountered. Such an expression may arise from a "diamond"-like diagram with the insertion $\Gamma = \gamma_5\,\sigma_{\mu\nu}$:
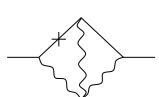
$$\longleftrightarrow \qquad \longrightarrow \qquad I^{\mu\nu\rho\sigma}(q) = \int \frac{d^4p\,d^4k}{(2\pi)^8}\,\frac{\overset{\circ}{k}{}^\mu\,\overset{\circ}{p}{}^\nu\,\overset{\circ}{p}{}^\rho\,\overset{\circ}{k}{}^\sigma}{(\hat{p}^2)^2\,\widehat{p+q}^2\,\widehat{k-p}^2\,\hat{k}^2\,\widehat{k+q}^2} \qquad \text{(B1)}$$

where q is the external momentum and

$$\hat{p}^\mu = 2\sin(\frac{p^\mu}{2}) \qquad , \qquad \hat{p}^2 = \sum_\mu 4\sin^2(\frac{p^\mu}{2}) \qquad , \qquad \overset{\circ}{p}{}^\mu = \sin(p^\mu) \qquad \text{(B2)}$$

No summation is implied over the indices μ, ν, ρ, σ.

----

[1] $\delta^{\mu\nu\rho\sigma} \equiv 1$, $\mu = \nu = \rho = \sigma$; $\delta^{\mu\nu\rho\sigma} = 0$, otherwise; $q^4 \equiv \sum_\mu (q^\mu)^4$.

From simple ultraviolet power counting on the term above, one can realize that the superficial degree of divergence is -8 and the degree of divergence in each of the two loops is -6 and -4. Thus, this term is not only superficially divergent but also contains a subdivergence in the right loop. All divergences are resolved by using a BPHZ procedure. The potential IR divergences, which may arise in intermediate steps, necessitate working in $D > 4$ dimensions as in [33]. Performing a BPHZ subtraction for the right loop, we split the integral into two parts:

$$I^{\mu\nu\rho\sigma}(q) \;=\; I^{\mu\nu\rho\sigma}_{\text{sub}}(q) + \int \frac{d^D p}{(2\pi)^D} \frac{\mathring{p}^\nu\,\mathring{p}^\rho}{(\hat{p}^2)^2\,\widehat{p+q}^2} \int \frac{d^D k}{(2\pi)^D} \frac{\mathring{k}^\mu\,\mathring{k}^\sigma}{(\hat{k}^2)^3} \tag{B3}$$

$$I^{\mu\nu\rho\sigma}_{\text{sub}}(q) \;\equiv\; \Bigg[\int \frac{d^D p\, d^D k}{(2\pi)^{2D}} \frac{\mathring{k}^\mu\,\mathring{k}^\sigma\,\mathring{p}^\nu\,\mathring{p}^\rho}{(\hat{p}^2)^2\,\widehat{p+q}^2\,\widehat{k-p}^2\,\hat{k}^2\,\widehat{k+q}^2}$$
$$-\int \frac{d^D p}{(2\pi)^D} \frac{\mathring{p}^\nu\,\mathring{p}^\rho}{(\hat{p}^2)^2\,\widehat{p+q}^2} \int \frac{d^D k}{(2\pi)^D} \frac{\mathring{k}^\mu\,\mathring{k}^\sigma}{(\hat{k}^2)^3} \Bigg] \tag{B4}$$

The last term in Eq. (B3) is a separable integral. The integral over momentum p is a standard primitively divergent integral (see, e.g., [35]), whose value contains only Lorentz invariant structures. The integral over momentum k does not depend on the external momentum q, and gives nonzero result only when the indices μ and σ are in the same direction. Thus, this term assumes the following structural form:

$$\int \frac{d^D p}{(2\pi)^D} \frac{\mathring{p}^\nu\,\mathring{p}^\rho}{(\hat{p}^2)^2\,\widehat{p+q}^2} \int \frac{d^D k}{(2\pi)^D} \frac{\mathring{k}^\mu\,\mathring{k}^\sigma}{(\hat{k}^2)^3} \qquad \longrightarrow \qquad \delta^{\mu\sigma}\left(a\,\delta^{\nu\rho} + b\,\frac{q^\nu\,q^\rho}{q^2} \right) \tag{B5}$$

In the remaining part of the original expression, we must still perform an extra subtraction, to cure the superficial divergence:

$$I_{\text{sub}}(q) = [I_{\text{sub}}(q) - I_{\text{sub}}(0)] + I_{\text{sub}}(0) \tag{B6}$$

According to the BPHZ procedure, the quantity $[I_{\text{sub}}(q) - I_{\text{sub}}(0)]$ is now UV-finite, and thus it equals the corresponding continuum expression. Consequently, once again, only Lorentz invariant structures arise:

$$[I_{\text{sub}}(q) - I_{\text{sub}}(0)] \;\longrightarrow\; a'\frac{q^\mu\,q^\nu\,q^\rho\,q^\sigma}{(q^2)^2} + \frac{b'}{q^2}\left(\delta^{\mu\nu}\,q^\rho\,q^\sigma + \delta^{\sigma\nu}\,q^\rho\,q^\mu + \delta^{\mu\rho}\,q^\nu\,q^\sigma + \delta^{\sigma\rho}\,q^\mu\,q^\nu\right)$$
$$+c'\,\delta^{\mu\sigma}\frac{q^\nu\,q^\rho}{q^2} + d'\,\delta^{\nu\rho}\frac{q^\mu\,q^\sigma}{q^2} + e'\left(\delta^{\mu\nu}\,\delta^{\rho\sigma} + \delta^{\sigma\nu}\,\delta^{\mu\rho}\right) + f'\,\delta^{\mu\sigma}\,\delta^{\nu\rho} \tag{B7}$$

The last part of the integral $I^{\mu\nu\rho\sigma}(q)$ (last term in Eq. (B6)) equals:

$$I^{\mu\nu\rho\sigma}_{\text{sub}}(0) = \int \frac{d^D p\, d^D k}{(2\pi)^{(2D)}} \frac{\mathring{k}^\mu\,\mathring{p}^\nu\,\mathring{p}^\rho\,\mathring{k}^\sigma}{(\hat{p}^2)^3\,(\hat{k}^2)^2}\left(\frac{1}{\widehat{k-p}^2} - \frac{1}{\hat{k}^2}\right) \tag{B8}$$

25

This q-independent integral could give rise to a structural form of the type $\delta^{\mu\nu\rho\sigma}$, which would spoil Lorentz invariance; however, this problem is avoided since the indices μ, ν in $I^{\mu\nu\rho\sigma}$ actually originate from the insertion $\Gamma = \gamma_5 \, \sigma_{\mu\nu}$. As a consequence, only the combination $I^{\mu\nu\rho\sigma} - I^{\nu\mu\rho\sigma}$ appears in the Feynman diagram, and no $\delta^{\mu\nu\rho\sigma}$ contribution survives. Thus, we are led to:

$$[I_{\text{sub}}^{\mu\nu\rho\sigma}(0) - I_{\text{sub}}^{\nu\mu\rho\sigma}(0)] \longrightarrow a \, (\delta^{\mu\rho} \, \delta^{\nu\sigma} - \delta^{\nu\rho} \, \delta^{\mu\sigma}) \tag{B9}$$

Having completed the whole procedure for the integral shown in Eq. (B1), we conclude that the only functional form that a four-index object (with the symmetries described above) can have reads:

$$\begin{aligned} I^{\mu\nu\rho\sigma}(q) - I^{\nu\mu\rho\sigma}(q) &= A\left(q^2\right) \, (\delta^{\mu\rho} \, \delta^{\nu\sigma} - \delta^{\nu\rho} \, \delta^{\mu\sigma}) \\ &+ \frac{B\left(q^2\right)}{q^2} \left(\delta^{\mu\rho} \, q^\nu \, q^\sigma - \delta^{\nu\rho} \, q^\mu \, q^\sigma \right) \\ &+ \frac{C\left(q^2\right)}{q^2} \left(\delta^{\mu\sigma} \, q^\nu \, q^\rho - \delta^{\nu\sigma} \, q^\mu \, q^\rho \right) \end{aligned} \tag{B10}$$

We emphasize again that, even though the above expression would be obvious in a continuum regularization, it is not so on the lattice, where one could have ended up with terms breaking Lorentz invariance.

Using similar considerations, we can prove that the two- and three-index expressions which appear in our calculation, will take the same structural form as in the continuum; i.e., they will be free of Lorentz non invariant contributions, which could be present a priori, such as $\delta^{\mu\nu} \, (q^\mu)^2/q^2$, $\delta^{\mu\nu\rho}$, etc.

Once we establish the structural form of the two-, three- and four-index integrals, we must compute the coefficients multiplying each tensor structure, such as the coefficients $A(q^2)$, $B(q^2)$, $C(q^2)$ of Eq. (B10). We illustrate the procedure by taking as an example the following two-index integral:

$$I^{\mu\nu}(q) = \int \frac{d^4p \, d^4k}{(2\pi)^8} \frac{\mathring{k}^\mu \, \mathring{p}^\nu \, (\mathring{k} \cdot \mathring{p})}{(\hat{p}^2)^2 \, \widehat{p+q}^2 \, \widehat{k-p}^2 \, \hat{k}^2 \, \widehat{k+q}^2} \tag{B11}$$

Along the same lines of reasoning as above, we conclude that the lattice integral $I^{\mu\nu}$ is of the same form as its continuum counterpart:

$$I^{\mu\nu}(q) = A \, \delta^{\mu\nu} + B \frac{q_\mu q_\nu}{q^2} \tag{B12}$$

The problem is now reduced to evaluating the coefficients A and B. Upon contracting the integral shown in Eq. (B12) with $\delta^{\mu\nu}$ and $q_\mu q_\nu$, we get:

$$I_1 \equiv \sum_{\mu\nu} \delta^{\mu\nu} I^{\mu\nu} = D A + B \tag{B13}$$

$$I_2 \equiv \sum_{\mu\nu} q_\mu q_\nu I^{\mu\nu} = A q^2 + B q^2 \tag{B14}$$

where D is the number of dimensions (on the lattice, $D = 4$). Once we evaluate the integrals I_1 and I_2, we are able to determine the quantities A and B through the following relations:

$$A = \frac{1}{3}\left(I_1 - \frac{1}{q^2} I_2\right) \quad , \quad B = \frac{1}{3}\left(\frac{4}{q^2} I_2 - I_1\right) \tag{B15}$$

Let us proceed with the evaluation of the integral I_1 by contracting $\delta^{\mu\nu}$ with Eq. (B11), keeping only terms of order $\mathcal{O}(q^0)$. At first, we aim to reduce the number of propagators appearing in the denominator by employing the following property, which is valid on the lattice:

$$\mathring{k} \cdot \mathring{p} = \frac{1}{2}\left[\widehat{k^2} + \widehat{p^2} - (\widehat{k-p})^2 - \frac{1}{2}\sum_\rho (\hat{k}^\rho)^2 \, (\hat{p}^\rho)^2\right] \tag{B16}$$

Omitting some intermediate steps, the resulting expression can be written as follows:

$$I_1 = I_a + I_b + I_c + I_d \tag{B17}$$

where

$$I_a = -\frac{1}{4}\int \frac{d^4p \, d^4k}{(2\pi)^8} \frac{(\mathring{k}\cdot\mathring{p})\sum_\rho(\hat{k}^\rho)^2 \, (\hat{p}^\rho)^2}{(\hat{p}^2)^2 \, \widehat{p+q}^2 \, \widehat{k-p}^2 \, \hat{k}^2 \, \widehat{k+q}^2} \tag{B18}$$

$$I_b = -\frac{1}{2}\sum_\rho \int \frac{d^4k}{(2\pi)^4} \frac{\mathring{k}^\rho}{\hat{k}^2 \, \widehat{k+q}^2} \cdot \int \frac{d^4p}{(2\pi)^4} \frac{\mathring{p}^\rho}{(\hat{p}^2)^2 \, \widehat{p+q}^2} \tag{B19}$$

$$I_c = \frac{1}{2}\int \frac{d^4p \, d^4k}{(2\pi)^8} \frac{\mathring{k}\cdot\mathring{p}}{\hat{k}^2 \, \widehat{k+q}^2 \, \hat{p}^2 \, \widehat{p+q}^2 \, \widehat{k-p}^2} \tag{B20}$$

$$I_d = \int \frac{d^4p \, d^4k}{(2\pi)^8} \frac{\mathring{k}\cdot\mathring{p}}{(\hat{p}^2)^2 \, \widehat{p+q}^2 \, \widehat{k+q}^2 \, \widehat{k-p}^2} = \frac{1}{2}\int \frac{d^4p \, d^4k}{(2\pi)^8} \frac{(k\overset{\circ}{-}q)\cdot(p\overset{\circ}{-}q)}{\hat{p}^2 \, \left(\widehat{p-q}^2\right)^2 \, \hat{k}^2 \, \widehat{k-p}^2} \tag{B21}$$

As can be seen from the expressions above, we have managed to reduce diamond-like expressions into simpler integrals. Integral I_a is IR convergent: one can set $q = 0$ and carry

out the integration numerically. Integral I_b, shown in Eq. (B19), is the product of two 1-loop integrals: The first one is well known and tabulated in [35], whereas the second, being UV-finite, equals its continuum analogue and can be solved by using the following formula found in Ref. [34]:

$$\int \frac{d^D p}{(2\pi)^D} \frac{\mathcal{P}_n(p)}{p^{2\alpha}\,(p-q)^{2\beta}} = \frac{(q^2)^{2-\varepsilon-\alpha-\beta}}{(4\pi^2)} \sum_{\sigma \geq 0} G(\alpha,\,\beta,\,n,\,\sigma)\, q^{2\sigma} \left[\frac{1}{\sigma!} \left(\frac{\Box_p}{4} \right)^\sigma \mathcal{P}_n(p) \right]_{p=q} \quad (B22)$$

where $\varepsilon = (4-D)/2$, $\Box_p \equiv \partial^2/\partial p_\mu \partial p_\mu$, and

$$G(\alpha,\,\beta,\,n,\,\sigma) = (4\pi)^\varepsilon \frac{\Gamma(\alpha+\beta-\sigma-2+\varepsilon)}{\Gamma(\alpha)\,\Gamma(\beta)} B(2-\varepsilon-\alpha+n-\sigma,\, 2-\varepsilon-\beta+\sigma)$$

$\Gamma(a)$ is the Gamma function and $B(\alpha,\beta) = \Gamma(\alpha)\,\Gamma(\beta)/\Gamma(\alpha+\beta)$ is the Beta function. $\mathcal{P}_n(p)$ is an arbitrary homogeneous polynomial in p: $\mathcal{P}_n(\lambda\,p) = \lambda^n \mathcal{P}_n(p)$. All UV-convergent integrals in our calculation can be treated using Eq. (B22), for various values of α, β, $\mathcal{P}_n(p)$ (and also Eq. (3.4) of [34] for diamond diagrams). Integral I_c of Eq. (B20) can be treated with one further application of Eq. (B16), leading to either IR convergent contributions or tabulated integrals (such as the scalar "eye" integral, Eq. (C.5) of [35]). Regarding the integral I_d, employing integration by parts, we find:

$$I_d = \frac{1}{2} \int \frac{d^4 p\, d^4 k}{(2\pi)^8} \frac{\sum_\rho \cos(k-q)^\rho}{\hat{p}^2 \,\widehat{p-q}^2\, \hat{k}^2\, \widehat{k-p}^2} - \frac{1}{2} \sum_\rho \partial_{q^\rho} \int \frac{d^4 p\, d^4 k}{(2\pi)^8} \frac{(k\overset{\circ}{-}q)^\rho}{\hat{p}^2 \,\widehat{p-q}^2\, \hat{k}^2\, \widehat{k-p}^2} \quad (B23)$$

Simple trigonometry on the first term in Eq. (B23): $\sum_\rho \cos(k-q)^\rho = 4 - \hat{k}^2/2 + \mathcal{O}(q)$ leads to the scalar eye diagram plus a simple, separable integral. The second term in Eq. (B23) is the derivative of a vector eye diagram, and can be resolved in two steps: (i) The integrand, $(k\overset{\circ}{-}q)^\rho/(\hat{p}^2 \,\widehat{p-q}^2\, \hat{k}^2\, \widehat{k-p}^2)$, after simple trigonometry and use of the symmetry $k \to p-k$, may be expressed in terms of superficially convergent and/or known divergent integrals, plus an integrand of the form $\overset{\circ}{p}{}^\rho/(\hat{p}^2 \,\widehat{p-q}^2\, \hat{k}^2\, \widehat{k-p}^2)$; (ii) the latter, upon contraction with $\overset{\circ}{q}{}^\rho$ and use of Eq. (B16), is expressed completely in terms of known integrals.

Some superficially convergent integrals, which contain subdivergences, often appear in various stages of our calculation. A simple prototype example is:

$$\frac{\sum_\rho (\hat{k}^\rho)^4}{\hat{p}^2 \,\widehat{p-q}^2\, \hat{k}^2\, \widehat{k-p}^2}$$

which is logarithmically divergent for $q \to 0$. In such cases, a subtraction of the form:

$$\frac{1}{\widehat{k-p}^2} = \frac{1}{\hat{k}^2} + \left(\frac{1}{\widehat{k-p}^2} - \frac{1}{\hat{k}^2} \right)$$

leads to known separable integrals, plus terms in which one can set $q = 0$ without appearance of divergences.

In conclusion, using the steps which we outlined above, we have managed to evaluate the integral I_1 of Eq. (B13), by reducing diamond-like structures into simpler ones, leading to expressions containing UV-finite integrals and standard primitively divergent integrals whose values are known. Using similar considerations, one can also evaluate the integral I_2 of Eq. (B14), which is needed up to order $\mathcal{O}(q^2)$. With the evaluation of these two integrals, we can fully determine the coefficients A and B of Eq. (B15), leading to the calculation of the original two-index integral. Let us point out that, throughout the whole procedure, the necessity to work in $D \neq 4$ dimensions does not emerge (It was only necessary in order to carry out demonstrations, such as Eqs. (B3-B9), leading to the conclusion: Eq. (B10)).

APPENDIX C: PER DIAGRAM RESULTS

In this appendix we present our perturbative results for the bare Green's functions, $\Sigma_\Gamma(g_\circ, a_{\mathrm{L}} q)$ (where $\Gamma = V, AV, T$), on a per diagram basis. Our results are expressed in terms of the bare coupling constant, $g_\circ$, the lattice spacing a_{L}, the external momentum, q and the clover parameter c_{SW}. For the sake of simplicity we have set $N_c = 3$ in two-loop expressions; at one-loop level the number of colors is left unspecified and the bare gauge parameter, $\alpha_\circ$, may take arbitrary values. In all cases, the number of flavors, N_f, can take arbitrary values.

Only one Feynman diagram, shown in Fig. 1, contributes to one-loop expressions. Our corresponding results for the three operators read:

$$
\begin{aligned}
\Sigma_{V, 1-loop}(g_\circ, a_{\mathrm{L}} q) \;=\; g_\circ^2 \frac{(N_c^2 - 1)}{N_c} \Bigg[& \gamma_\mu \Big(-\frac{\alpha_\circ}{32\pi^2} \log\left(a_{\mathrm{L}}^2 q^2\right) + 0.0151728775487(3)\, \alpha_\circ \\
& + 0.01258087658(1) - 0.007905256548(1)\, c_{\mathrm{SW}} \\
& + 0.0027043227859(1)\, c_{\mathrm{SW}}^2 \Big) \\
& + \frac{q_\mu \slashed{q}}{q^2} \Big(-\frac{1}{16\pi^2}\, \alpha_\circ \Big) \Bigg]
\end{aligned}
\tag{C1}
$$

$$
\begin{aligned}
\Sigma_{AV, 1-loop}(g_\circ, a_{\mathrm{L}} q) \;=\; g_\circ^2 \frac{(N_c^2 - 1)}{N_c} \gamma_5 \Bigg[& \gamma_\mu \Big(-\frac{\alpha_\circ}{32\pi^2} \log\left(a_{\mathrm{L}}^2 q^2\right) + 0.0151728775487(3)\, \alpha_\circ \\
& - 0.002685425493(8) + 0.007905256548(1)\, c_{\mathrm{SW}} \\
& - 0.0027043227859(1)\, c_{\mathrm{SW}}^2 \Big) \\
& + \frac{q_\mu \slashed{q}}{q^2} \Big(-\frac{1}{16\pi^2}\, \alpha_\circ \Big) \Bigg]
\end{aligned}
\tag{C2}
$$

$$
\begin{aligned}
\Sigma_{T, 1-loop}(g_\circ, a_{\mathrm{L}} q) \;=\; g_\circ^2 \frac{(N_c^2 - 1)}{N_c} \gamma_5\, \sigma_{\mu\nu} \Bigg[& \frac{1 - \alpha_\circ}{32\pi^2} \log\left(a_{\mathrm{L}}^2 q^2\right) + 0.01200659055973(9)\, \alpha_\circ \\
& + 0.00118313174(2) - 0.0052701710(1)\, c_{\mathrm{SW}} \\
& - 0.001820704300(1)\, c_{\mathrm{SW}}^2 \Bigg]
\end{aligned}
\tag{C3}
$$

The contribution to the bare Green's functions from the ℓ-th two-loop diagram, can be written in the following form:

$$
\begin{aligned}
\Sigma_{V, 2-loop}^{(\ell)}(g_\circ, a_{\mathrm{L}} q) \;=\; g_\circ^4 N_f^k \Bigg[& \gamma_\mu \sum_i c_{\mathrm{SW}}^i \Big(\frac{v_{1,i}^{(\ell)}}{1152\pi^4} \log^2\left(a_{\mathrm{L}}^2 q^2\right) + v_{2,i}^{(\ell)} \log\left(a_{\mathrm{L}}^2 q^2\right) + v_{3,i}^{(\ell)} \Big) \\
& + \frac{q_\mu \slashed{q}}{q^2} \sum_i c_{\mathrm{SW}}^i \Big(\frac{v_{1,i}^{(\ell)}}{288\pi^4} \log\left(a_{\mathrm{L}}^2 q^2\right) + v_{4,i}^{(\ell)} \Big) \Bigg]
\end{aligned}
\tag{C4}
$$

$$\Sigma^{(\ell)}_{AV,\,2-loop}(g_\circ, a_{\mathrm{L}}\, q) \;=\; g_\circ^4\, N_f^k\, \gamma_5 \left[\gamma_\mu \sum_i c_{\mathrm{SW}}^i \left(\frac{w^{(\ell)}_{1,i}}{1152\pi^4} \log^2\left(a_{\mathrm{L}}^2 q^2\right) + w^{(\ell)}_{2,i} \log\left(a_{\mathrm{L}}^2 q^2\right) + w^{(\ell)}_{3,i} \right) \right.$$

$$\left. + \frac{q_\mu \slashed{q}}{q^2} \sum_i c_{\mathrm{SW}}^i \left(\frac{w^{(\ell)}_{1,i}}{288\pi^4} \log\left(a_{\mathrm{L}}^2 q^2\right) + w^{(\ell)}_{4,i} \right) \right] \tag{C5}$$

$$\Sigma^{(\ell)}_{T,\,2-loop}(g_\circ, a_{\mathrm{L}}\, q) = g_\circ^4\, N_f^k\, \gamma_5\, \sigma_{\mu\nu} \left[\sum_i c_{\mathrm{SW}}^i \left(\frac{x^{(\ell)}_{1,i}}{1152\pi^4} \log^2\left(a_{\mathrm{L}}^2 q^2\right) + x^{(\ell)}_{2,i} \log\left(a_{\mathrm{L}}^2 q^2\right) + x^{(\ell)}_{3,i} \right) \right]$$
$$\tag{C6}$$

where the index ℓ runs over all contributing two-loop diagrams. The dependence on c_{SW} is polynomial of degree up to 4 ($i = 0, \cdots, 4$). The number of flavors, N_f, is raised to the power k where, of course, $k = 1$ only for diagrams 8 and 9 of Fig. 2, since they are the only diagrams containing a closed fermion loop; the remaining diagrams have $k = 0$. The coefficients $v^{(\ell)}$, $w^{(\ell)}$ and $x^{(\ell)}$ are numerical constants obtained upon evaluating each two-loop Feynman diagram. In Tables I-II, III-IV and V-VI, we present our results for $v^{(\ell)}$, $w^{(\ell)}$ and $x^{(\ell)}$, respectively, with accuracy up to 10 decimal places.

In the case of the singlet Axial-Vector operator, it turns out that the only additional diagram contributing to $\Sigma^{(\ell)}_{AV,singlet}(a_{\mathrm{L}}q)$ is diagram 4 of Fig. 3. It is a straight forward exercise to recover the bare matrix element; starting from $Z^{L,RI'}_{AV,\,singlet}$ (Eq. (35)) and $Z^{L,RI'}_{\psi}$ (Eq. (29)), one can employ the RI' renormalization condition, Eq. 12, to extract the corresponding matrix element.

ACKNOWLEDGMENTS

TABLE I: Contribution of two-loop diagrams to $\Sigma_{V,2-loop}^{(\ell)}$ ($\ell = 1-14$)

ℓ	i	$\mathrm{v}_{1,i}^{(\ell)}$	$\mathrm{v}_{2,i}^{(\ell)}$	$\mathrm{v}_{3,i}^{(\ell)}$	$\mathrm{v}_{4,i}^{(\ell)}$
	0	0	0.0010901413	-0.00955549(5)	0.0021802826
1	1	0	0	0.0089908(2)	0
	2	0	0	-0.00522028(9)	0
	0	0	0	0.00230566(3)	0
2	1	0	0	0	0
	2	0	0	-0.000041360(2)	0
	0	0	-0.0004010149	0.01183022(2)	-0.0008020299
3-7	1	0	0	-0.00738844(3)	0
	2	0	0	0.00260794(1)	0
	0	0	0.0000534687	-0.0003947(1)	0.0001069374
	1	0	0	0.00032545(2)	0
8-9	2	0	0	-0.00077830(1)	0
	3	0	0	0.000389303(9)	0
	4	0	0	-0.000146063(2)	0
	0	0	-0.0017442261	0.0152888292	-0.0034884521
10-11	1	0	0	-0.0043548025	0
	2	0	0	0.0014897419	0
	0	0	0	0	0
12	1	0	0	0.000063005(3)	0
	2	0	0	-0.000061816(2)	0
	0	0	0.0000390267	-0.000161967(5)	0.0000780534
13	1	0	0.0001255891	-0.00099763(1)	0.0002511781
	2	0	-0.0002000264	0.00009461(1)	-0.0004000527
	3	0	0	-0.000046762(1)	0
	0	0	0	0.00045044(3)	0
14	1	0	0	-0.00147021(3)	0
	2	0	0	-0.000043209(1)	0
	3	0	0	0.000057664(2)	0

TABLE II: Contribution of two-loop diagrams to $\Sigma_{V,2-loop}^{(\ell)}$ ($\ell = 15-20$)

ℓ	i	$v_{1,i}^{(\ell)}$	$v_{2,i}^{(\ell)}$	$v_{3,i}^{(\ell)}$	$v_{4,i}^{(\ell)}$
	0	27	-0.0020904154	0.0061629(1)	-0.00418077(4)
15	1	0	-0.0005507191	-0.0010101(1)	-0.0011014381
	2	0	0.0001759227	0.00026474(6)	0.0003518455
	3	0	0	0.000424491(6)	0
	0	0	0.0000390267	-0.000342083(4)	0.0000780534
16	1	0	0.0001255891	0.001157216(6)	0.0002511781
	2	0	-0.0002000264	0.00178325(2)	-0.0004000527
	3	0	0	-0.000076152(1)	0
	0	0	-0.0000356458	-0.000049925(1)	0.00001874(2)
	1	0	0	0.000198131(2)	0
17	2	0	0	-0.000064731(4)	0
	3	0	0	-0.0000161812(2)	0
	4	0	0	0.0000032674	0
	0	-1	0.0000558195	0.000098634(7)	0.00002159(5)
	1	0	-0.0000211097	-0.000057416(3)	-0.0000422194
18	2	0	0.0000249033	-0.000179175(1)	0.0000498067
	3	0	0	0.0000335005(3)	0
	4	0	0	0.0000077358(2)	0
	0	-8	0.0002681483	-0.0086175(2)	-0.0000340358
	1	0	0.0003206506	0.0144022(6)	0.0006413012
19	2	0	0.0001992266	0.00454038(9)	0.0003984533
	3	0	0	0.00128588(2)	0
	4	0	0	-0.00047870(1)	0
	0	4	-0.0008031274	0.00453973(4)	-0.00103589(2)
	1	0	0.0001779933	-0.00234305(6)	0.0003559866
20	2	0	-0.0000608900	0.00090217(4)	-0.0001217801
	3	0	0	0.000065108(4)	0
	4	0	0	0.0000428543(8)	0

TABLE III: Contribution of two-loop diagrams to $\Sigma_{AV,2-loop}^{(\ell)}$ $(\ell = 1-14)$

ℓ	i	$w_{1,i}^{(\ell)}$	$w_{2,i}^{(\ell)}$	$w_{3,i}^{(\ell)}$	$w_{4,i}^{(\ell)}$
	0	0	0.0010901413	-0.004299380(2)	0.0021802826
1	1	0	0	-0.0089908(2)	0
	2	0	0	0.00522028(9)	0
	0	0	0	-0.00010270(1)	0
2	1	0	0	0	0
	2	0	0	0.000041360(2)	0
	0	0	-0.0004010149	-0.00177094(2)	-0.0008020299
3-7	1	0	0	0.00738844(3)	0
	2	0	0	-0.00260794(1)	0
	0	0	0.0000534687	-0.0000143(1)	0.0001069374
	1	0	0	-0.00019712(2)	0
8-9	2	0	0	0.00001658(1)	0
	3	0	0	-0.000389303(9)	0
	4	0	0	0.000146063(2)	0
	0	0	-0.0017442261	0.0068790161	-0.0034884521
10-11	1	0	0	0.0043548025	0
	2	0	0	-0.0014897419	0
	0	0	0	0	0
12	1	0	0	-0.000063005(3)	0
	2	0	0	0.000061816(2)	0
	0	0	0.0000390267	0.00017234(2)	0.0000780534
13	1	0	0.0001255891	0.00172937(5)	0.0002511781
	2	0	-0.0002000264	-0.00147678(5)	-0.0004000527
	3	0	0	0.000046762(1)	0
	0	0	0	0.000203052(3)	0
14	1	0	0	0.00057021(3)	0
	2	0	0	0.00010067(1)	0
	3	0	0	-0.000057664(2)	0

TABLE IV: Contribution of two-loop diagrams to $\Sigma_{AV,2-loop}^{(\ell)}$ $(\ell = 15-20)$

ℓ	i	$w_{1,i}^{(\ell)}$	$w_{2,i}^{(\ell)}$	$w_{3,i}^{(\ell)}$	$w_{4,i}^{(\ell)}$
	0	27	-0.0020904154	0.0019129(1)	-0.00418077(4)
15	1	0	-0.0005507191	0.0048214(1)	-0.0011014381
	2	0	0.0001759227	-0.00100389(6)	0.0003518455
	3	0	0	-0.000424491(6)	0
	0	0	0.0000390267	-0.0001539166(3)	0.0000780534
16	1	0	0.0001255891	0.00125957(2)	0.0002511781
	2	0	-0.0002000264	0.001151401(6)	-0.0004000527
	3	0	0	0.000076152(1)	0
	0	0	-0.0000356458	-0.000281627(7)	0.0005068330
	1	0	0	0.000060887(2)	0
17	2	0	0	0.000050595(4)	0
	3	0	0	-0.000006587(2)	0
	4	0	0	-0.0000046598(4)	0
	0	-1	0.0000558195	0.000050308(7)	0.00002159(5)
	1	0	-0.0000211097	-0.000226495(3)	-0.0000422194
18	2	0	0.0000249033	0.000086519(1)	0.0000498067
	3	0	0	-0.0000336128(3)	0
	4	0	0	-0.0000077358(2)	0
	0	-8	0.0002681483	-0.0206450(5)	-0.0000340358
	1	0	0.0003206506	0.0253960(7)	0.0006413012
19	2	0	0.0001992266	0.0064762(2)	0.0003984533
	3	0	0	-0.00199356(7)	0
	4	0	0	-0.000442050(6)	0
	0	4	-0.0004593941	0.00110429(4)	-0.00034842(2)
	1	0	-0.0001779933	0.00063376(6)	-0.0003559866
20	2	0	0.0000608900	-0.00029572(4)	0.0001217801
	3	0	0	-0.000201975(4)	0
	4	0	0	0.0000060939(8)	0

TABLE V: Contribution of two-loop diagrams to $\Sigma^{(\ell)}_{T,2-loop}$ ($\ell = 1-14$)

ℓ	i	$x^{(\ell)}_{1,i}$	$x^{(\ell)}_{2,i}$	$x^{(\ell)}_{3,i}$
	0	0	0	-0.0045414(8)
1	1	0	0	0.0059942(3)
	2	0	0	0.0035149(4)
	0	0	0	0.0010537(2)
2	1	0	0	0
	2	0	0	-0.0012514(2)
	0	-15	0.0028583491	0.001177(1)
3-7	1	0	0	-0.00492566(5)
	2	0	0	-0.001583088(1)
	0	2	-0.0000803010	-0.0000461(3)
	1	0	0.0000426116	0.00022585(9)
8-9	2	0	-0.0002519813	-0.00021615(4)
	3	0	0	0.00024528(3)
	4	0	0	0.000058928(5)
	0	0	0	0.0072658787
10-11	1	0	0	-0.0029032016
	2	0	0	-0.0010029792
	0	0	0	0
12	1	0	0	0.0003050(1)
	2	0	0	0.0000039204(9)
	0	0	0	-0.00002584(1)
13	1	0	0	0.00029039(5)
	2	0	0	-0.0008905(1)
	3	0	0	-0.000030105(2)
	0	0	0	0.0002775(1)
14	1	0	0	-0.0015909(4)
	2	0	0	0.00030041(3)
	3	0	0	-0.000030400(2)

TABLE VI: Contribution of two-loop diagrams to $\Sigma^{(\ell)}_{T,2-loop}$ ($\ell = 15-20$)

ℓ	i	$x^{(\ell)}_{1,i}$	$x^{(\ell)}_{2,i}$	$x^{(\ell)}_{3,i}$
	0	0	0	0.0017380(8)
15	1	0	0	-0.0011468(3)
	2	0	0	-0.00090530(9)
	3	0	0	0.000054081(9)
	0	0	0	-0.00016259(4)
16	1	0	0	0.0007288(1)
	2	0	0	0.0007569(1)
	3	0	0	-0.000050771(5)
	0	0	0.0000356458	0.00003599(7)
	1	0	0	0.000034379(6)
17	2	0	0	-0.00007614(2)
	3	0	0	-0.000023760(4)
	4	0	0	-0.0000109914(9)
	0	0	0.0000356457	0.0001341(1)
	1	0	0	-0.00022585(1)
18	2	0	0	-0.00003143(2)
	3	0	0	0.0000069846(4)
	4	0	0	-0.0000045409(4)
	0	0	0	0.026645(7)
	1	0	0	-0.04180(1)
19	2	0	0	-0.00994(5)
	3	0	0	0.0049633(8)
	4	0	0	0.00067162(8)
	0	0	0	0.0010004(2)
	1	0	0	-0.0071228(5)
20	2	0	0	-0.00010774(3)
	3	0	0	0.000068781(9)
	4	0	0	0.0000163351(2)

[1] A. Skouroupathis and H. Panagopoulos, Phys. Rev. **D76** (2007) 094514 [arXiv:0707.2906].

[2] J.A. Gracey, Nucl. Phys. **B662** (2003) 247 [hep-ph/0304113].

[3] G. Martinelli and Y. Zhang, Phys. Lett. **123B** (1983) 433.

[4] S. Aoki, K. Nagai, Y. Taniguchi and A. Ukawa, Phys. Rev. **D58** (1998) 074505 [hep-lat/9802034].

[5] S. Capitani et al., Nucl. Phys. **B593** (2001) 183 [hep-lat/0007004].

[6] J.B. Zhang et al., Phys. Rev. **D72** (2005) 114509 [hep-lat/0507022].

[7] D. Bećirević et al., Phys. Rev. **D74** (2006) 034501 [hep-lat/0605006].

[8] Y. Aoki, C. Dawson, J. Noaki and A. Soni, Phys. Rev. **D75** (2007) 014507 [hep-lat/0607002].

[9] D. Galletly et al., Phys. Rev. **D75** (2007) 073015 [hep-lat/0607024].

[10] R. Sommer, *Non-perturbative QCD: renormalization, O(a)-improvement and matching to Heavy Quark Effective Theory*, hep-lat/0611020.

[11] M. Della Morte, P. Fritzsch and J. Heitger, JHEP **0702** (2007) 079 [hep-lat/0611036].

[12] F. Di Renzo, V. Miccio, L. Scorzato and C. Torrero, PoS LAT2006 (2006) 156 [hep-lat/0609077].

[13] F. Di Renzo, V. Miccio, L. Scorzato and C. Torrero, Eur. Phys. J. **C51** (2007) 645 [hep-lat/0611013].

[14] F. Di Renzo, L. Scorzato and C. Torrero, PoS LAT2007 (2007) 240 [arXiv:0710.0552].

[15] Q. Mason et al., Phys. Rev. **D73** (2006) 114501 [hep-ph/0511160].

[16] D.D. Dietrich, F. Sannino and K. Tuominen, Phys. Rev. **D72** (2005) 055001 [hep-ph/0505059].

[17] P. Kovtun, M. Unsal and L. G. Yaffe, JHEP **0706** (2007) 019 [hep-th/0702021].

[18] M. García Pérez and A. González-Arroyo, JHEP **0611** (2006) 091 [hep-th/0609058].

[19] G. Cossu et al., PoS LAT2006 (2006) 069 [hep-lat/0609049].

[20] F. Basile, A. Pelissetto and E. Vicari, PoS LAT2005 (2005) 199 [hep-lat/0509018].

[21] A. González-Arroyo and R. Kirchner, JHEP **0601** (2006) 029 [hep-lat/0507036].

[22] J. Engels, S. Holtmann and T. Schulze, Nucl. Phys. **B724** (2005) 357 [hep-lat/0505008].

[23] T. Ryttov and F. Sannino, Phys. Rev. **D76** (2007) 105004 [arXiv:0707.3166].

[24] D.D. Dietrich and F. Sannino, Phys. Rev. **D75** (2007) 085018 [hep-ph/0611341].

[25] B. Sheikholeslami and R. Wohlert, Nucl. Phys. **B259** (1985) 572.

[26] G. Martinelli et al., Nucl. Phys. **B445** (1995) 81 [hep-lat/9411010].

[27] E. Franco and V. Lubicz, Nucl. Phys. **B531** (1998) 641 [hep-lat/9803491].

[28] K.G. Chetyrkin and A. Rétey, Nucl. Phys. **B583** (2000) 3 [hep-ph/9910332].

[29] J.C. Collins, *Renormalization*, Cambridge University Press, 1984.

[30] K.G. Chetyrkin and A. Rétey, *Three-loop Three-Linear Vertices and Four-Loop MOM beta functions in massless QCD* [hep-ph/0007088].

[31] G.'t Hooft and M. Veltman, Nucl. Phys. **B44** (1972) 189.

[32] S.A. Larin and J.A.M. Vermaseren, Phys. Lett. **B303** (1993) 334 [hep-ph/9302208]; S.A. Larin, Phys. Lett. **B303** (1993) 113 [hep-ph/9302240, containing an extra section] and private communication.

[33] H. Kawai, R. Nakayama and K. Seo, Nucl. Phys. **B189** (1981) 40.

[34] K.G. Chetyrkin and F.V. Tkachov, Nucl. Phys. **B192** (1981) 159.

[35] M. Lüscher and P. Weisz, Phys. Lett. **B349** (1995) 165 [hep-lat/9502001]; M. Lüscher and P. Weisz, Nucl. Phys. **B452** (1995) 234 [hep-lat/9505011].

[36] H. Panagopoulos, A. Skouroupathis and A. Tsapalis, Phys. Rev. **D73** (2006) 054511 [hep-lat/0601009].

[37] A. Bode and H. Panagopoulos, Nucl. Phys. **B625** (2002) 198 [hep-lat/0110211].

[38] M. Lüscher et al., Nucl. Phys. **B491** (1997) 323 [hep-lat/9609035].

[39] R. Frezzotti et al., Nucl. Phys. Proc. Suppl. **83** (2000) 941 [hep-lat/9909003].

[40] R. Frezzotti and G.C. Rossi, JHEP **0410** (2004) 070 [hep-lat/0407002].

[41] S. Catterall et. al., JHEP **0811** (2008) 009 [arXiv:0807.0792].

[42] L. Del Debbio, A. Patella and C. Pica, *Higher representations on the lattice: numerical simulations. SU(2) with adjoint fermions* [arXiv:0805.2058].
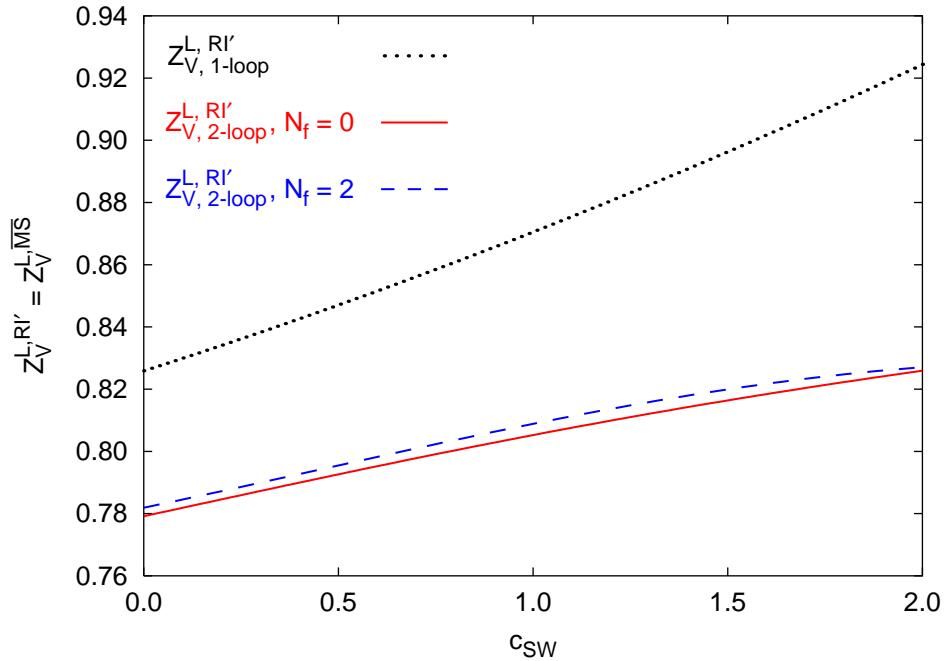
FIG. 4: $Z_V^{L,RI'}(a_L\bar{\mu}) = Z_V^{L,\overline{MS}}(a_L\bar{\mu})$ versus c_{SW} ($N_c = 3$, $\bar{\mu} = 1/a_L$, $\beta_o = 6.0$). Results up to 2 loops are shown for $N_f = 0$ (solid line) and $N_f = 2$ (dashed line); one-loop results are plotted with a dotted line.
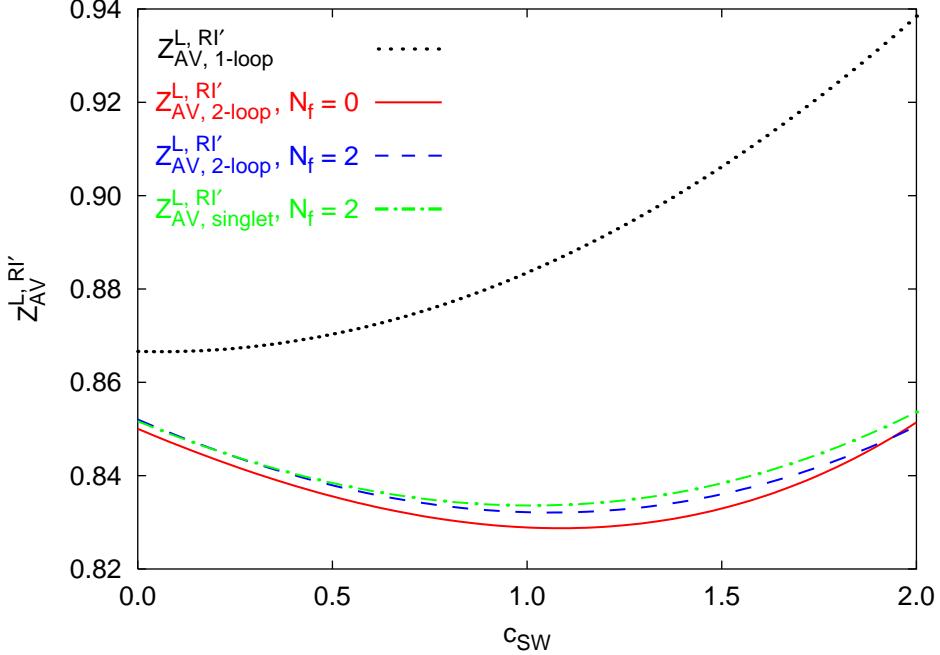
FIG. 5: $Z_{AV}^{L,RI'}(a_{\rm L}\bar{\mu})$ versus $c_{\rm SW}$ ($N_c = 3$, $\bar{\mu} = 1/a_{\rm L}$, $\beta_{\rm o} = 6.0$). Results up to 2 loops, for the flavor nonsinglet operator, are shown for $N_f = 0$ (solid line) and $N_f = 2$ (dashed line); 2-loop results for the flavor singlet operator, for $N_f = 2$, are plotted with a dash-dotted line; one-loop results are plotted with a dotted line.
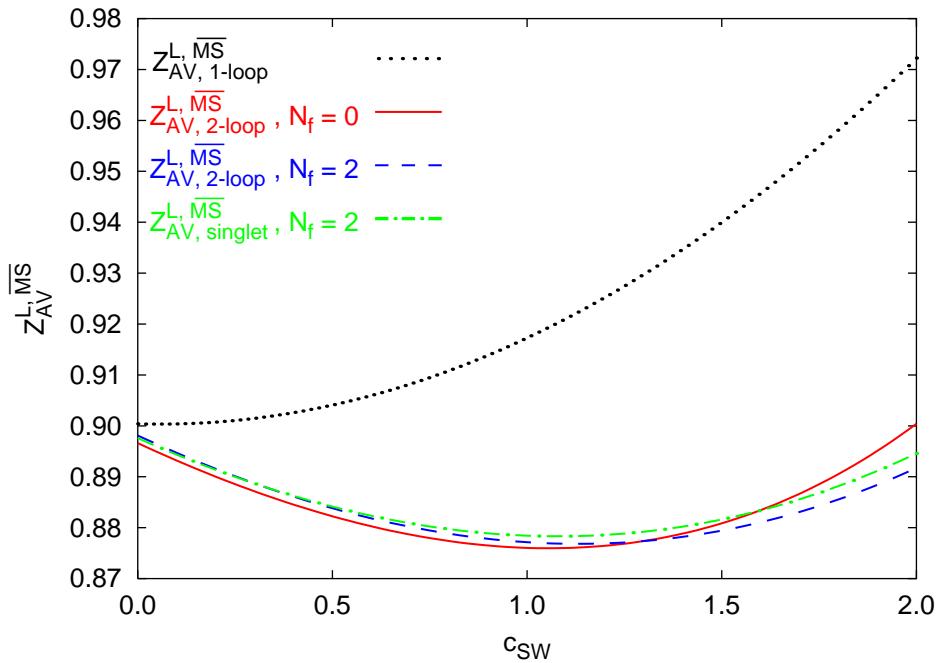
FIG. 6: $Z_{AV}^{L,\overline{MS}}(a_{\rm L}\bar{\mu})$ versus $c_{\rm SW}$ ($N_c = 3$, $\bar{\mu} = 1/a_{\rm L}$, $\beta_{\rm o} = 6.0$). Same notation as in Fig. 5.
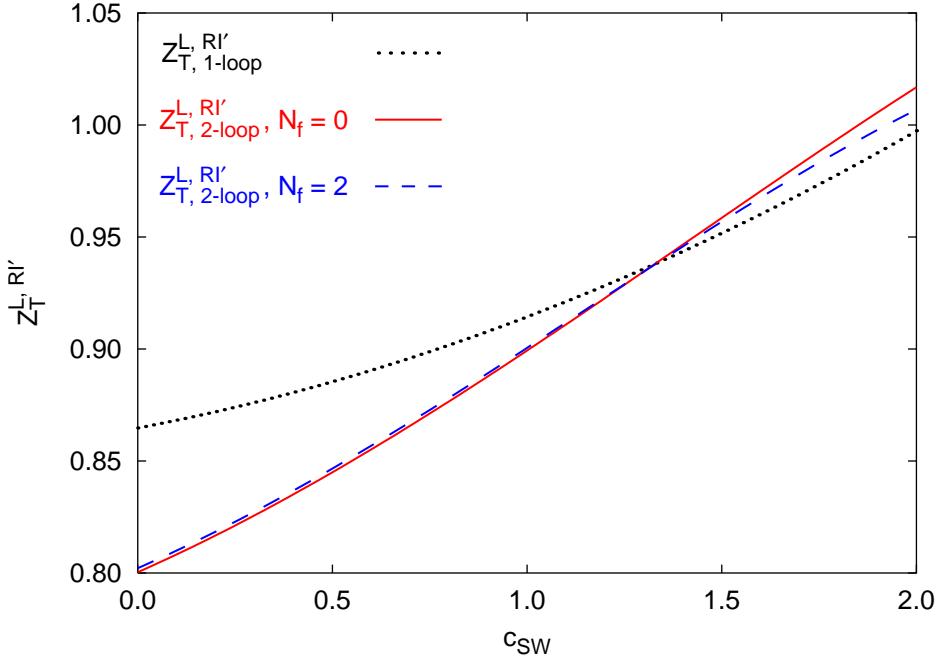
FIG. 7: $Z_T^{L,RI'}(a_{\rm L}\bar{\mu})$ versus $c_{\rm SW}$ ($N_c = 3$, $\bar{\mu} = 1/a_{\rm L}$, $\beta_{\rm o} = 6.0$). Results up to 2 loops are shown for $N_f = 0$ (solid line) and $N_f = 2$ (dashed line); one-loop results are plotted with a dotted line.
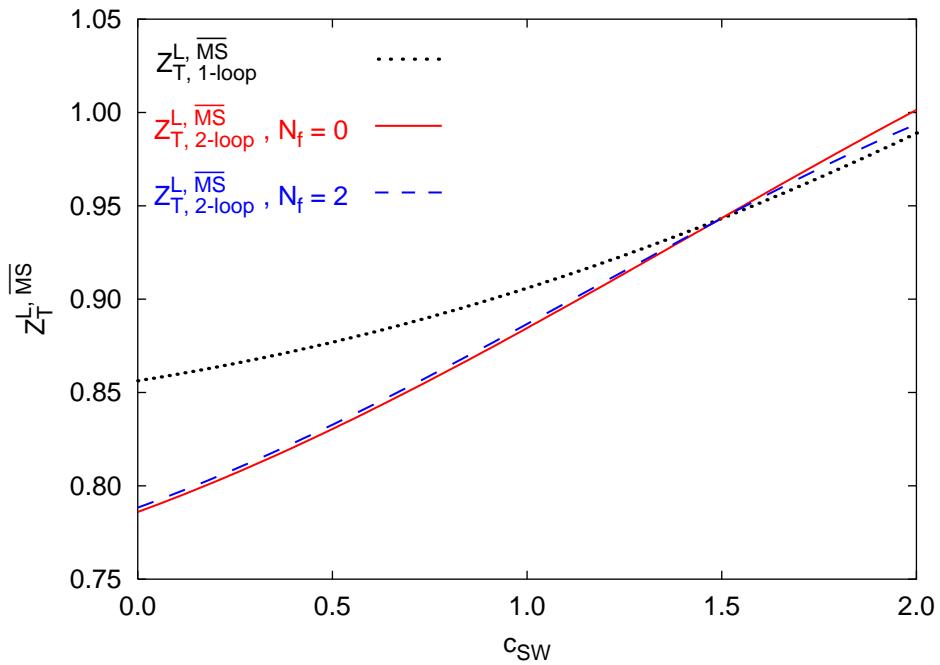

FIG. 8: $Z_T^{L,\overline{MS}}(a_{\rm L}\bar{\mu})$ versus $c_{\rm SW}$ ($N_c = 3$, $\bar{\mu} = 1/a_{\rm L}$, $\beta_{\rm o} = 6.0$). Same notation as in Fig. 7.
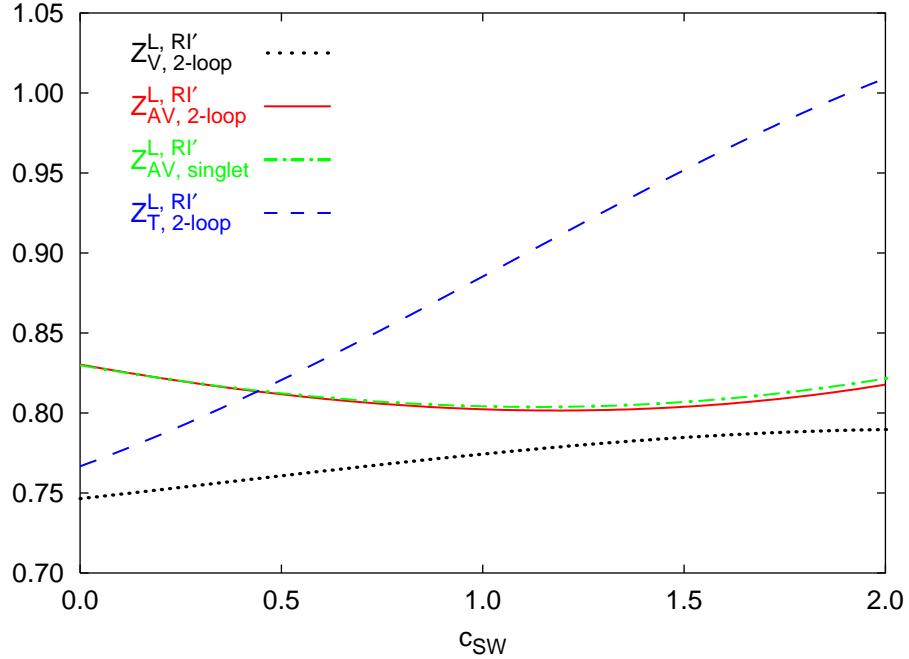
FIG. 9: $Z_V^{L,RI'}$ (dotted line), $Z_{AV}^{L,RI'}$ (solid line), $Z_{AV,singlet}^{L,RI'}$ (dash-dotted line) and $Z_T^{L,RI'}$ (dashed line) up to 2 loops, versus c_{SW} ($N_c = 3$, $\bar{\mu} = 1/a_L$, $N_f = 2$, $\beta_o = 5.3$).
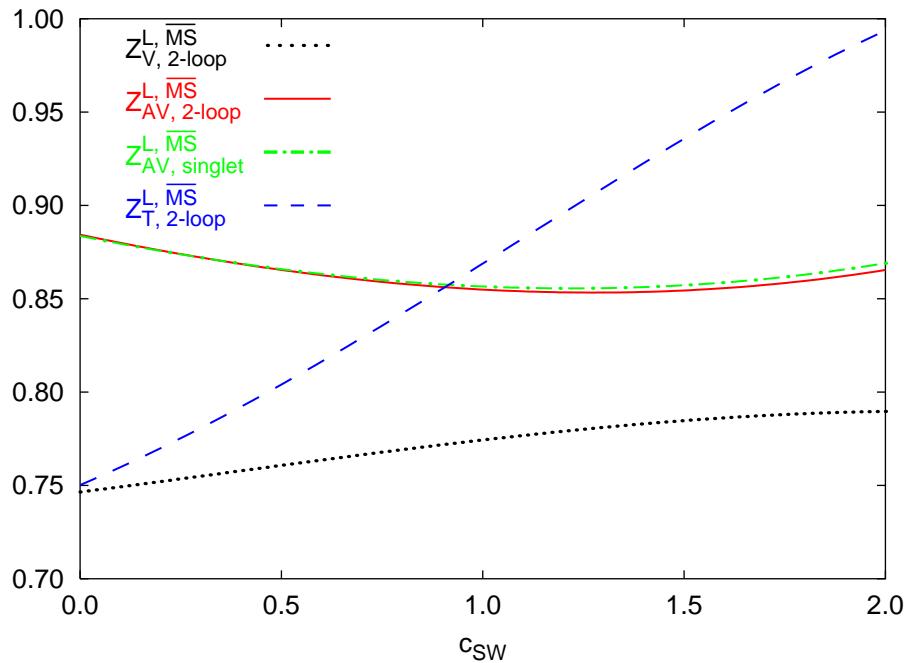

FIG. 10: $Z_V^{L,\overline{MS}}$ (dotted line), $Z_{AV}^{L,\overline{MS}}$ (solid line), $Z_{AV,singlet}^{L,\overline{MS}}$ (dash-dotted line) and $Z_T^{L,\overline{MS}}$ (dashed line) up to 2 loops, versus c_{SW} ($N_c = 3$, $\bar{\mu} = 1/a_L$, $N_f = 2$, $\beta_o = 5.3$).